INTERSPECIES EXCHANGE MUTAGENESIS OF THE FVII EGF-1 DOMAIN

INTERSPECIES EXCHANGE MUTAGENESIS OF

THE FIRST EPIDERMAL GROWTH FACTOR-LIKE DOMAIN OF

COAGULATION FACTOR VII

By

VANESSA JANE WILLIAMSON, B.Sc.

A Thesis

Submitted to the School of Graduate Studies

in Partial Fulfillment of the Requirements

for the Degree

Master of Science

McMaster University

MASTER OF SCIENCE (2000) McMaster University
(Biology) Hamilton, Ontario

TITLE: Interspecies Exchange Mutagenesis of the First Epidermal Growth Factor-

Like Domain of Coagulation Factor VII

AUTHOR: Vanessa Jane Williamson, B.Sc. (Hons), University of Guelph

SUPERVISOR: Dr. Bryan Clarke

SUPERVISORY COMMITTEE: Dr. M.A. Blajchman
Dr. W.P. Sheffield
Dr. B. White

NUMBER OF PAGES: xii, 136

ABSTRACT

A high degree of structural and sequence homology exists between the EGF-1 domains of the vitamin K-dependent coagulation factors, as well as between the EGF-1 domains of individual vitamin K-dependent coagulation factors from various species. Through studies of protein evolution it has been determined the conserved amino acid residues observed are essential for protein structure while the variable residues have been implicated in specific protein-protein interactions. In the case of FVII, this interaction is the high affinity binding of its cofactor, TF, which initiates the extrinsic pathway of coagulation. 43% of the contact area of the FVII molecule in the FVIIa•TF complex is located within the FVII EGF-1 domain.

A series of human FVII variants have been constructed in which the EGF-1 domain has been exchanged, either in its entirety or as single amino acid substitutions, with that of the mouse or rabbit. These species were chosen as it had previously been shown that plasma from mouse or rabbit, when combined with human TF, was able to clot at a significantly greater rate than homologous human plasma. We hypothesized that through these exchanges it might be possible to generate a human FVII variant with increased TF binding.

Of the FVII variants generated, 2 human FVII point mutants have shown an increased affinity for human TF after transient expression. A75D and T83K exhibited TF binding at 200% and 150%, respectively, of that seen with wild-type human FVII. Both A75D and T83K exhibited clotting and amidolytic activity that was proportionally

increased, with respect to TF binding. Computer-generated structures of these variants predict an additional hydrogen bond between the FVII and TF molecules likely to be responsible for the increased TF affinity in the T83K mutant. Intramolecular forces within the FVII molecule are predicted to have caused a conformational change with the A75D mutation which has lead to its increased TF binding.

The greater affinity for TF exhibited by the human FVII point mutants A75D and T83K, as compared to wild-type human FVII, is an important step toward the creation of new class of competitive inhibitors of coagulation which are specifically directed towards its initial stage, rather than later in the cascade. However, more study is needed to determine the ability of either of these mutants to compete against each other for TF both *in vitro* and *in vivo*. If either mutant is successful, it can then be active site inhibited by site-directed mutagenesis or through the use of chloromethyl ketones, in order to decrease its clotting and amidolytic activity.

ACKNOWLEDGEMENTS

TABLE OF CONTENTS

3.0   RESULTS

4.0   DISCUSSION

LIST OF FIGURES

LIST OF TABLES

LIST OF SYMBOLS AND ABBREVIATIONS

α	alpha
β	beta
γ	gamma
Å	angstrom
°	degrees
A	absorbance
AT	antithrombin
AP	alkaline phosphatase
Arg	arginine
Asp	aspartic acid
BHK	baby hamster kidney
bp	base pair
BSA	bovine serum albumin
CACB	carbonate antigen coating buffer
CAT	chloramphenicol acetyl transferse
cDNA	complementary deoxyribonucleic acid
CGM	complete growth media
Cys	cysteine
ddH_2O	double distilled water
DMEM	Dulbeco's Modified Eagles medium
DNA	deoxyribonucleic acid
E. coli	*Escherichia coli*
EDTA	ethylene diamine tetraacetic acid
EGF	epidermal growth factor
ELISA	enzyme linked immunosorbent assay
EtOH	ethanol
FCS	fetal calf serum
FIX	factor IX
FIXa	activated FIX
FVII	factor VII
FVIIa	activated FVII
FX	factor X
FXa	activated FX
Gla	γ-carboxyglutamic acid
Gln	glutamine
Gly	glycine
HEK	human embryonic kidney
hFVII	human factor VII
IgG	immunoglobulin G
Ile	isoleucine

IPTG	β-D-isopropyl-thiogaalactopyranoside
KAc	potassium acetate
kb	kilobase
kcal	kilocalorie
K_d	dissociation constant
kDa	kilodalton
LB	Luria broth
Leu	leucine
Lys	lysine
mol	mole
μL	microliter
mL	milliliter
mM	millimolar
NaAc	sodium acetate
NaCl	sodium chloride
NaOH	sodium hydroxide
ng	nanogram
nm	nanometer
nM	nanomolar
NMR	nuclear magnetic resonance
NPP	normal pooled plasma
OD	optical density
O/N	overnight
PBS	phosphate buffered saline
PCR	polymerase chain reaction
pd hFVII	plasma derived human factor VII
Phe	phenylalanine
PNPP	paranitrophenyl phosphate
P/S	penicillin/streptomycin
PT	prothrombin
rFVII	recombinant factor VII
RT	room temperature
SDS	sodium dodecyl sulphate
S-S	disulphide bond
sTF	soluble tissue factor
TEMED	N,N.N',N'-tetramethylethylenediamine
TF	tissue factor
TFPI	tissue factor pathway inhibitor
Thr	threonine
TM	transfection media
(v:v)	volume:volume
(w:v)	weight:volume
X-gal	5-bromo-4-chloro-3-indolyl-β-galactoside

1.0   INTRODUCTION

1.1   Human Coagulation Factor VII

Human blood coagulation factor VII, commonly referred to as factor VII, is a 50

kDa, 406 amino acid, single chain serine protease zymogen. Its gene is located at

chromosomal position 13q34, approximately 2.8 kb upstream of the FX gene, and

comprises eight exons spanning a total of 13 kb (1, 8, 12, 13, 33, 49). It is found in

human plasma at an average concentration of 500 ng/mL (~10nM), and although greater

than 98% of the FVII circulating is in the zymogen form, approximately 4 ng/mL of the

activated serine protease FVIIa, can be detected (27, 33). But despite being the

proteolytically activated form of its zymogen, FVIIa shows no appreciable enzymatic

activity until brought into contact with its cofactor, TF.

FVII has a multi-domain structure (see Figure 1), a quality that it has in common

with many other proteins involved in coagulation (6, 11,19, 33). At its N-terminus there

is a γ–carboxyglutamic acid-containing (Gla) domain, followed by an aromatic stack

region (residues 37 to 46). Next are two epidermal growth factor-like domains (residues

46 to 152), EGF-1 and EGF-2, which are connected by a short, poorly formed helix, that

may act as a hinge region. The catalytic, or serine protease domain, is found at the C-

terminal end of the molecule (1, 6, 19, 33).

FVII contains nine Ca^{2+}-binding sites, seven of low affinity and two of high

affinity. The seven low affinity sites, each with a K_d of approximately 1mM, are found in

the Gla domain, and the binding of calcium to these sites assists in the binding of FVII to

anionic phospholipid membranes. The high affinity Ca^{2+}-binding sites ($K_d \sim 150\ \mu M$) are found in the EGF-1 and the serine protease domain, and are associated with both the binding of FVII to TF, and with amidolytic activity (33). The FVII EGF-1 high affinity site coordinates a calcium ion between six oxygen atoms from five different amino acid residues within EGF-1 (Asp46, Gly47, Gln49, Asp63 (which donates 2 oxygen atoms), and Gln64), and an oxygen atom from a surrounding water molecule (1, 26). The single high affinity Ca^{2+} binding site of the EGF-1 domain is a feature that the FVII EGF-1 domain shares with that of FIX and FX. The same residues are also shown by NMR to coordinate the calcium atom in FIX and FX (1, 20, 41, 49).

As with many of the coagulation factors, FVII is synthesized in the liver before being secreted into the blood. Because of this, it is synthesized with a 38 amino acid pre-pro leader sequence at its N-terminal end. The pre-sequence (residues −36 to −24) is essential for secretion of the protein. The pro-sequence (residues −17 to −1) is a signal for the carboxylation of the N-terminal glutamic acid residues, and contains highly conserved residues found in other vitamin K-dependent proteins. FVII undergoes a post-translational vitamin K-dependent modification to generate ten γ-carboxylic glutamic acid residues, at amino acids 6, 7, 14, 16, 19, 20, 25, 26, 29 and 35, at the N-terminus of the molecule (6, 19, 33, 52).

FVII also possesses two O-glycosylated serine residues in the EGF-1 domain, at amino acid positions 52 and 60 (4, 23, 33), as well as two N-glycosylated asparagines in the catalytic domain, at amino acid positions 145 and 322 (33). The function of these glycosylations is not completely understood, though they were initially predicted to play

a role in the optimal function or the plasma half-life of FVII. Mutational studies in which the serine residues at amino acids 52 and 60 were changed to alanine, showed a reduced clotting activity of these variants compared to wild-type, though amidolytic activity was virtually unchanged (23). Both mutations also showed decreased association constants, as compared to wild-type human FVII, though the dissociation constants were unchanged (4). These results suggest that the sugar moieties attached to the serine residues at amino acids 52 and 60 in FVIIa provide unique structural elements that are important for the rapid association of FVII with TF.

In addition to its low plasma concentration, FVII has a very short half-life. At only three to four hours, this is the shortest half-life observed of any of the coagulation factors (52). Consequently, FVII deficiency is a common occurrence. Zymogen levels can rapidly decline during a state of liver disease, as well as when therapeutic oral anticoagulants are taken which act as vitamin K antagonists. FVII deficiency is associated with either variable bleeding, or more rarely, as well as paradoxically, thrombotic manifestations. On the other hand, elevated FVII levels can also cause clinical problems, and have been specifically associated with an increased risk of cardiovascular disease (52).

Figure 1: Domain Structure of Human FVII. Amino acid sequence and structure of prepro-factor VII. The prepro leader sequence is the first 60 amino acids (numbered -60 to -1). The Gla and epidermal growth factor-like domains are located within residues 1-152 and constitute the light chain of FVIIa. The FXa cleavage site of FVII is between amino acids 152 and 153 and is indicated with an arrow. The serine protease domain contains the latter 254 amino acid residues. Disulphide bonds are indicated. Adapted from Hagen et al., 1987.

GROWTH FACTOR DOMAINS

S L L A
Y G D
G E G V
H C-C S
N G G C-C R T P T V E Y P C G K I P I L E K R N ◆145
E C E Q Y-C S A
E N V C-C S R K S
F E G R N C I L Q D D H T K P
A P L F C-C E T H K G
C C I Y S Q L Q
P Q N G G S
S S A C-C β 63
A Q

Factor Xa
152 R
1

C L P V V H
R E P L V V H
F T H E G L V A I
F A L T R E S F Q P V L L T N R N N L L V/Q
L Q G W G S V L S F R V I L R L H D E S L L W P
A G R L D I A L L D D G C-C P
L A G R L D V R S Q E D G K I K N W R N C-L E G K
41
M E L L A A S V V S A A C-C L G
M V L K V G D S P N◆170 V V W I T N I L L T T
R S Q O L C-C F M D G K C-C G Q G W S V I Y T
N V P R L M T Q D A G Y S D G S K D S A T V G H F G V
90 D H

CATALYTIC DOMAIN

A T H Y R G T W Y L
H P T G
P G G I
G G S V
192 S D G K C-C G Q G W S V I
P 254
COOH

GLA DOMAIN

Q C-C T R T L S G P R L γ γ L F A N ⓐⓑ R R R H L V G H A E E Q T V F V R H P G P
γ γ K
6 14
Processing Protease

PRE-PRO LEADER

SEQUENCE

NH2
-60 M V S Q A L R L L C L L L G L Q G C L A A G G V A K A S S G G S
NH2
P K W W P M D
R T R

1.2   Tissue Factor

TF is an integral membrane single-chain glycoprotein that is associated

with phospholipid and found in most tissues other than the normal endothelium.

It is 293 amino acid residues in length, with a preceding 32 amino acid signaling

peptide (6, 27, 33, 36). The protein is composed of three structural domains; a

cytoplasmic region that constitutes the C-terminal end of the protein and is

associated with the cell membrane, a transmembrane region, and an N-terminal

extracellular domain (32). Soluble TF comprises the later of these regions (amino

acid residues 1-219), and it is this domain which has been implicated in the tight

binding with FVII (1, 6).

The solution structure of sTF is known, and is very similar to that of the

interferon-γ receptor, as well as other cytokine receptors (1, 17). It is this

structural similarity which suggests a true receptor function of TF. sTF consists

of two fibronectin type III-like repeats, TF1 and TF2, which are arranged end to

end. The interface between these two domains generates a rigid structure with an

"elbow" angle of approximately 120°(1).

True to its receptor function, TF has been implicated in a number of

biological functions not directly related to coagulation, including tumor metastasis

and angiogenesis (32). The FVII•TF complex has also been reported to play a

role in transmembrane signaling, though its precise role in this is not yet known

(1). In coagulation however, the roles of TF are much clearer. TF functions as a

cell surface binding protein and as a cofactor for FVIIa. TF is usually confined to

cells that are not in direct contact with the blood stream, including the adventitia of the vessel wall and atherosclerotic plaques. Upon vessel injury or plaque rupture, TF is exposed to the circulation. At this time it acts as a cell surface binding protein, capable of complexing with FVII. Once exposed to the blood, FVII and FVIIa rapidly bind TF in a calcium-dependent manner, forming the bimolecular FVIIa•TF complex on the phospholipid membrane (33, 36). This interaction has an affinity of < 1 nM, with protein-protein interactions contributing 12-14 kcal/mol of the free energy of binding (43). It is this complex which exhibits FVIIa enzymatic activity, and initiates the blood coagulation cascade.

Certain disease states also exist, during which TF is inappropriately exposed on the surface of cells, including heart disease, cancer, and other severe infections (17, 32). When this occurs, FVII binds TF, becomes activated, and forms inappropriate and unregulated blood clots in many of the small blood vessels of the body, such as those associated with the heart, lungs, and brain. More times than not, these clots become thrombotic and life threatening.

1.3   The FVII•TF Complex

As already mentioned, FVII is virtually inactive in plasma. But upon complexing with its cell surface cofactor, TF, FVII is activated to its serine protease form, FVIIa. This activation is a result of the proteolytic cleavage of the Arg_{152}-Ile_{153} peptide bond within FVIIa, and occurs rapidly upon complexing of the two proteins (1, 6, 8). The proteolysis reaction occurs in the presence of many

naturally occurring plasma enzymes, including FVIIa, FXIIa, FIXa, FXa, and thrombin. The result of this cleavage is the generation of a two-chain molecule, with a 152 amino acid N-terminal light chain, and a 254 amino acid C-terminal heavy chain, connected by a S-S bridge between cysteine residues at amino acid positions 135 and 262 (1, 6, 33).

All four domains of the FVIIa molecule have been implicated in the binding to TF, including the Gla, EGF-like, and catalytic domains (8, 9, 21, 35). Many studies suggest that an interaction with the EGF-1 domain provides the major driving force. In 1992 it was demonstrated in our laboratory, through the use of a monoclonal antibody specific for the EGF-1 domain of FVII, that the EGF-1 was essential for TF binding (9). It has also been demonstrated in our laboratory that the two naturally occurring FVII EGF-1 domain mutants, N57D and R79Q, have strongly reduced TF binding (8, 28).

O'Brien et al. further examined the R79Q mutant using surface plasmon resonance studies. They showed that R79Q had reduced activity with respect to wild type FVII, as well as reduced affinity for TF. Its association rate constant was only 1/5 that of wild-type, while its dissociation rate constant was relatively unchanged, ultimately resulting in a decreased affinity of FVII for TF (35). Dickinson et al. also published a study showing the key residues in the FVII EGF-1, with respect to TF binding. Alanine scanning mutagenesis was employed to show the critical roles of FVII residues Gln64, Ile69, Phe71 and Arg74 in TF binding (15). Many other biochemical studies have also been conducted,

implicating the EGF-1 domain of FVII as that which plays a primary role of FVII

interaction with TF (6, 7, 21, 25, 26). Although this evidence is very convincing,

it was not conclusive until the realization of the crystal structure of the FVII•TF

complex.

The greatest insight into the specific structure of the FVIIa•TF complex

came with the publication by Banner *et al.,* in 1996, of the crystal structure of

active site inhibited FVIIa in complex with sTF figure (Figure 2). The structure is

determined at a 2.0 Å resolution, is approximately 115 Å long and 40-50 Å in

diameter, and shows all four domains of the FVIIa molecule including the

calcium binding sites. FVII adopts an extended conformation when in complex

with TF and wraps itself around TF, orienting its Gla domain proximal to, and its

catalytic domain distal to, the cell membrane region (1, 17).

In complex with FVII, TF maintains a structure very similar to that which

it has in its free form, with a few slight changes (1). There is a small shift in the

TF loop including the residues Leu_{133} and Phe_{140}, helping to bring these two

residues in contact with FVIIa. There is also some disorder seen in amino acid

residues 135-138, 153-164 and 181-183. The "binding epitope" of the TF

molecule is seen as a stripe running along the whole length of TF, which imposes

upon the otherwise flexible FVIIa molecule, a specific overall conformation by

binding in three distinct areas. The lower right hand side of TF2 binds the Gla

domain of FVIIa, the front central region at the TF1/TF2 domain boundary binds

the EGF-1 domain, and the top of TF1 binds the EGF-2 and catalytic domain.

These three regions have a total buried surface area upon complex formation of 1800 Å (1). The C-terminus of TF adheres to the phospholipid cell membrane (1, 17). The structure and spatial location of the active-site region provide an insight into the way that TF turns FVIIa into a fully functional enzyme (1, 17).

Although the EGF-1 domain comprises only a small portion of the FVIIa molecule, approximately 11% of the full length FVII, with respect to sequence (19), it accounts for approximately 43% of the contact area between the EGF-1 domain of FVII and sTF (1). The major hydrophobic interactions between TF and the EGF-1 domain of FVII are (with T representing the TF molecule and E representing the EGF-1 domain of FVII): Phe140T, Leu133T and Arg131T with Phe71E; Leu133T, Lys120T, Thr17T with Ile69E; and Ile22T with Arg79L. In addition, the Lys20 residue of TF points into the hole just below the Cys72-Cys81 disulphide bond of FVII (1). An extensive network of hydrogen bonds is formed between TF and the EGF-1 domain of FVII. Well-determined hydrogen bonds exist between TF and 3 residues within the EGF-1 domain of FVII. Cys70 and Glu77 each make one hydrogen bond with TF1, Gly78 makes 2, and Arg79 makes 3 hydrogen bonds with the TF1 domain of TF. The only hydrogen bond found to form between TF2 and the EGF-1 domain of FVII is at FVII Gln64. The arginine residue at amino acid 79 of FVII is particularly important in the formation of the FVIIa•TF complex, as it participates in both hydrophobic and hydrogen bonding interactions (1).

Figure 2: Crystal Structure of the FVIIa•TF Complex. The structure of soluble TF in complex with FVIIa, generated using Swiss-Pdb Viewer, version 3.51, and the coordinates from the Protein Data Base file 1DAN.pdb. The FVII light chain is shown in white and the catalytic domain of FVII is shown in red. The tissue factor chain is shown in blue. + symbols in pink represent calcium ions, and γ-carboxylic glutaminc acid residues are shown in green. The sugar moieties in the EGF-1 domain of FVII at amino acids 52 and 60 are shown in orange and dark blue, respectively. Disulphide bonds are illustrated in yellow. The active site inhibitor , D-Phe-L-Phe-Arg chloromethyl ketone, is located in the catalytic domain and is shown as a large yellow area.
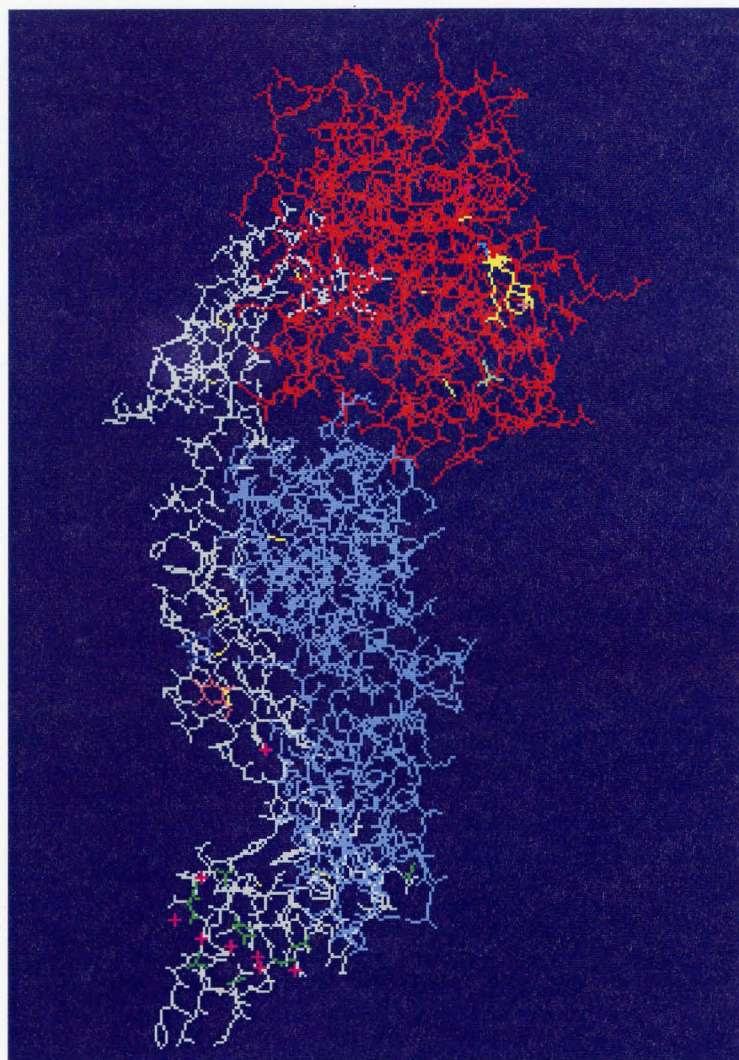
1.4   The Human Blood Coagulation Cascade

1.4.1   Initiation of Coagulation

Human blood coagulation is driven by the formation of a series of complexes between serine protease coagulation factors and their corresponding membrane bound cofactors (Figure 3). This includes, but is not limited to, the complexing of FVIIa with TF, FIXa with FVIIIa, and FXa with FVa (11, 33). There are two pathways of coagulation, the extrinsic pathway and the intrinsic pathway. It is the tight binding between FVII and TF, upon vascular injury and in the presence of calcium and phospholipid membrane, which triggers the former of these two paths. After TF binding, FVII is activated by proteolytic cleavage at a single site, and in turn activates the serine protease zymogens FIX and FX into their enzymatically active forms FIXa and FXa. FIXa activates FX to FXa, and FXa activates prothrombin to thrombin. This ultimately leads to fibrinogen cleavage and the generation of a fibrin clot. In addition, thrombin activates FV and FVII to FVa and FVIIIa, respectively. The activation reaction in each of these plasma proteins involves the cleavage of one or two internal peptide bonds (11, 33). Additionally, thrombin activates the thrombin receptor on platelets that results in platelet activation and aggregation. Fibrin formation and platelet activation are key events in normal haemostasis as well as in thrombotic disorders, and both are triggered by the formation of the FVII•TF complex (11).

Figure 3: The Coagulation Cascade. The extrinsic and extrinsic pathways of coagulation are shown. The coagulation cascade is initiated following vascular injury when TF is exposed to the blood. The extrinsic pathway is triggered as FVII and TF complex, in the presence of calcium and phospholipid. This leads to the activation of FX to FXa, prothrombin to thrombin, fibrinogen to fibrin, and ultimately the formation of a fibrin clot. Reprinted with permission from Enzyme Research Laboratories, Inc.

Contact Factor Pathway
(Intrinsic Pathway)

Tissue Factor Pathway
(Extrinsic Pathway)

"Tissue Damage"

Kallikrein ← Prekallikrein

HK | HK

XII → XIIa

(VIIa)

XI | Ca++

C-I inhibitor

Tissue Factor

TFPI → Xa

VIIa ← VII

XIa (VIIa)

IX | Ca++

IXa

X | Ca++ PL

VIII — IIa → VIIIa

Protein S | Protein S

II | Ca++ PL

APC

IIa | V | IIa → Va

Xa | Ca++ PL

IIa ← Heparin Cofactor II

Antithrombin

Protein C inhibitor

Thrombomodulin

Protein C

Fibrinogen → Fibrin Monomer

Fibrin Polymer

XIIIa | Ca++

Fibrin Clot

FDP

Fibrinolysis

Plasminogen

UK,SK tPA

PAI-1

Plasmin

α-2 Antiplasmin

Protein Concentrations

Component	Molecular Weight	Plasma Concentration µg/ml	Plasma Concentration µM
Fibrinogen (I)	330,000	3000	9.09
Prothrombin (II)	72,000	100	1.388
Factor V	330,000	10	0.03
Factor VII	50,000	0.5	0.01
Factor VIII	330,000	0.1	0.0003
Factor IX	56,000	5	0.08928
Factor X	58,800	8	0.13605
Factor XI	160,000	5	0.031
Factor XII	80,000	30	0.375
Factor XIII	320,000	10	0.03125
Protein C	62,000	4	0.0645
Protein S	69,000	10(free)	0.1449
Protein Z	62,000	2.2	0.0355
Prekallikrein	86,000	50	0.5814
HK	110,000	70	0.6363
Fibronectin	450,000	300	0.6667
Antithrombin III	58,000	290	5
Plasminogen	90,000	120	1.333
Urokinase	53,000	0.1	0.001887
Heparin Cofactor II	66,000	90	1.3636
Alpha$_2$-Antiplasmin	63,000	60	0.9524
Protein C Inhibitor	57,000	4	0.0702
Alpha$_2$-Macroglobulin	725,000	2100	2.8966

1.4.2 Regulation of Coagulation

There are many mechanisms by which the coagulation pathways are physiologically regulated. Various serine proteases positively regulate the process and a variety of protease inhibitors exist which slow the generation of a fibrin clot. In tandem these compounds are essential to maintaining a healthy balance of thrombosis and haemostasis (11). Protease inhibitors exist which act at various stages of the coagulation cascade, but for the purpose of this discussion, these will be limited to those which affect the FVIIa•TF complex.

The most predominant physiological regulator of the extrinsic pathway of coagulation is TFPI (11, 12, 38). TFPI is a member of the Kunitz inhibitor family, which blocks fibrin formation by forming an inactive complex with FVIIa/TF/FXa. As a consequence of the existence of TFPI, the extrinsic pathway is probably short lived. TFPI is synthesized on the surface of endothelial cells and platelets and circulates in the plasma associated with these lipoproteins. It is potentiated by the administration of heparin or thrombin, but due to its very low concentration (~2 nM), even with the administration of these compounds TFPI is unable to completely block coagulation, but rather regulates it (12). Another protease inhibitor of the coagulation cascade is AT. AT is known to inactivate thrombin as well as factors IXa, Xa, and IXa. The inactivation of these clotting factors is a result of the formation of a 1:1 complex between AT and the activated cofactor, and is greatly enhanced in the presence of heparin. It has been suggested that AT can effectively inhibit the FVIIa•TF complex also, though this observation is controversial (14). Non-physiological inhibitors of the FVIIa•TF complex

also exist, including aprotinin, monoclonal antibodies, derivatives of FVII, and active site

inhibited chemical derivatives of FVIIa (12, 14).

When clinically regulating coagulation only two anticoagulants have widespread

use, coumarins and heparins (11). Coumarins act by interfering with γ carboxylation,

thereby impairing the function of the vitamin-K dependent proteins. These include both

procoagulants such as factors VIIa, IXa and Xa, and thrombin, as well as the

anticoagulants such as activated protein C and protein S. Heparins, as already mentioned,

enhance FXa and thrombin inhibition by AT. Though effective, both coumarins and

heparins face clinical limitations, as they act in a non-selective manner and have

difficulty in maintaining a healthy balance between thrombosis and haemostasis (14).

1.5   Protein Evolution

1.5.1   Evidence for the Assembly of Coagulation Proteases from Modules

It is an increasingly accepted notion that many proteins are constructed from

various modules, each of which can be identified by a consensus sequence that is often

related to the exon structure of the gene (16, 37, 38, 39). Characterization of both the

amino acid sequences and the genes of various coagulation proteases, as well as those

involved in fibrinolysis and complement activation, has revealed that their catalytic

regions are homologous with those of the trypsin-like serine proteases. In addition to this

catalytic region, these complex proteases have large segments inserted between their

signal peptide and their zymogen activation domain within the trypsin-homolog region.

This feature distinguishes the proteases of coagulation and fibrinolysis from the simpler

proteases of the trypsin family, including pancreatic proteases, glandular kallikreins, and

mast cell proteases, which possess only a signal peptide attached to the N-terminal end of the enzyme region (37, 38).

Structure-function studies of the coagulation proteases have revealed that in general these non-catalytic segments mediate binding to macroscopic structures, cofactors, substrates, and inhibitors, all of which regulate the activity and activation of these enzymes, and ultimately the cascades of coagulation and fibrinolysis (37, 38). The non-catalytic regions are organized into a variety of structural-functional domains, including, but not limited to, kringles, vitamin K-dependent calcium binding domains, and EGF-like domains (37). The latter two of these 2 modules are observed in the FVII molecule. Earliest studies conducted with respect to individual structural domains of the complex proteases were done on isolated kringle domains (38). Because they have been the most extensively studied regions, observations about these modules have provided most of the initial insight into the modular evolution of the proteases, and the hypothesis that the non-catalytic segments of the regulatory proteases are constructed from modules. More current studies have extended the observations seen with respect to the structure and function of kringle domains to the other structural modules of multidomain proteins, including the EGF-like domain.

Kringle domains have been shown to correspond to independent structural-functional units that are also autonomous with respect to folding. The folding of kringle 4 of plasminogen is a very well directed process with native intermediates dominant in the folding pathway (38). This suggests that the remarkably simple, well-directed folding pathway of kringles reflects the extreme importance of folding autonomy of modules in

multidomain proteins. The independence of these modules may be a consequence of their evolutionary autonomy and they may have evolved outside of the family of serine proteases and then have been fused to the catalytic regions individually. Evidence of modular evolution can also be seen with tissue plasminogen activator, where a region has been identified which is homologous to the finger domains (type I domains) of fibronectin. Fibronectin is an extracellular matrix protein, which aside from its homology to tissue plasminogen activator in this respect, is unrelated to the serine proteases (38). It has been found that EGF is derived from a precursor that is not related to the proteases, suggesting that EGF-like modules of proteases could be borrowed from other proteins (37, 38).

These initial observations suggest that the common ancestor of the regulatory proteases is similar to the simple trypsin-like proteases, and that all regulatory modules have been individually inserted between the signal peptide and zymogen activation domains (37, 38). Comparison of the evolutionary history of the individual modules with the gene structure of the protease domains has confirmed this assumption and allowed for the reconstruction of the assembly process. Many of the more recently sequenced proteases of coagulation and fibrinolysis have also been found to be mosaics assembled from modules. Though this may appear a somewhat general statement, it is further supported by the observation that most nonprotease constituents of the plasma effector systems, components of the extracellular matrix, and receptors, have also shown to be assembled from modules. Ultimately this demonstrates the underlying importance of the evolutionary strategy of modular assembly. The acquisition of new modules can give

novel binding specificities to the recipient protein that can lead to dramatic changes in its regulation and targeting. In modular proteins much distinct binding specificity may also coexist, making these proteins ideal for regulatory networks where multiple interactions are necessary. These concepts can be exploited in protein engineering when it is desirable to create novel interactions that change the regulation, specificity or targeting of the protease (38).

1.5.2 Module Shuffling by Exon Shuffling

The hypothesis of modular assembly implies that the gene pieces encoding the module display a remarkable mobility during evolution, and that these modules are capable of undergoing repeated insertions, tandem duplications, and exchanges. To explain this unusual mobility it must be assumed that special features exist, causing their genes to contribute to the frequent genetic rearrangements. Exon shuffling is one theoretical mechanism that can be held responsible for the modular shuffling (16, 37, 38, 39). The correlation which exists between the previously mentioned mosaic structure of TPA and the exon-intron organization of its gene, provided the first conclusive evidence for modular exchange by exon shuffling. In the TPA gene, introns have been found exactly where homology predicted module boundaries, indicating the possibility of exon shuffling as the mechanism by which these otherwise unrelated proteins acquired finger domains homologous to fibronectin. Additional studies of the exon-intron organization of the genes of the regulatory proteases, as well as other mosaic proteins containing related modules, have revealed that in general introns are found at the module boundaries.

It has also been found that the gene structures of all trypsin-like serine proteases possess a phase 1 intron at the boundary of the protease region and the non-protease part. A phase 1 intron is one that splits the reading frame between the first and second nucleotide of a codon. This suggests that the common ancestor of these proteases that also possessed a phase 1 intron in this position and, according to the hypothesis, this intron of the ancestral protease was the recipient of modules during the assembly process (37, 38).

1.5.3   Structure-Function Correlation of Modules

The same gross architecture has been retained by the EGF-like domains of the vitamin K-dependent coagulation factors VII, X and IX (11, 20, 49), but apparently has diverged enough that each binds different proteins or low-molecular weight compounds. From this, it may be predicted that if the amino acid sequences of EGF-like domains possessing different binding functions are compared, the residues involved directly in the diverse binding functions may show great variability, whereas the residues found in all or most of these domains are essential for the autonomous folding and structure of EGF-like domains (39). The conserved residues then serve as a scaffold and the variable binding sites are determined predominantly by variable peptide regions not reserved for the residues that determine folding. Binding sites of individual EGF-like domains may therefore be predicted from regions noted for their variability. NMR spectroscopy and X-ray crystallography of EGF-like domains has confirmed these suggestions, showing conserved residues are typically involved in homologous interactions that stabilize the structure of the module (38, 39).

Ultimately, modules may show great variation in function while retaining the capacity to acquire the same three-dimensional architecture. Comparison of the sequences of modules with diverse binding specificities can help identify the structurally important regions of the proteins and localize the regions that are likely to determine binding specificity. This information may be used to predict the three-dimensional structure of modules and to guide site-directed mutagenesis and protein engineering of modules.

1.5.4   Epidermal Growth Factor-Like Domains

EGF-like domains are modules found in a wide variety of extracellular proteins, including those associated with blood coagulation, fibrinolysis, complement activation, cell adhesion, and neural development. These domains may exist as either a single copy or as multiple copies, and are often found in association with other protein modules. They exhibit a diverse range of biological functions, but their major role is in the mediation of protein-protein interactions (5, 41, 51). EGF-like domains also serve as spacers, orienting the active site of serine proteases. Typically these structural motifs contain 40-50 amino acid residues, including six conserved cysteines forming three disulphide bridges, paired in a 1-3, 2-4 and 5-6 manner. The main features of this folding pattern are the generation of a central two-stranded antiparallel β-sheet that is connected to the N-terminal part of the EGF-like domain by two of the S-S bridges (3, 41). The final S-S bridge connects the central part of the molecule to the C-terminal portion of the EGF-like domain, which also contains a short stretch of two-stranded antiparallel β-sheet (41).

Despite the fact that there is a high degree of both structural and functional homology in EGF-like domains, even between species, each possesses its own degree of specificity. Considerable evidence has shown that if many of the residues in the EGF-1 domain of FVII are altered, or even if the whole domain is exchanged for the EGF-1 domain from another vitamin K-dependent protein, TF binding will be greatly decreased, if not abolished (6). Similar observations have been made with the bovine species, where it has been shown that the EGF-1 and Gla domains are essential in the generation of the TF•FVII complex (21).

1.6 Homologies of Plasma Proteins

1.6.1 Implications of Homologies in Protein Structure and Function

Identification of homologies between the multidomain regulatory proteases is useful for structure-function studies, especially where no X-ray crystallographic data exists. Since the gross architecture of related modules of different proteins is conserved, the structure of modules may be predicted on the basis of homology (11, 18, 38, 49). The domain organization and key structural features of regulatory proteases can then be predicted if the architecture of homologous domains and modules is known. When combined with information on the spatial arrangement and interactions of modules obtained by neutron scattering, X-ray scattering studies, and cross-linking experiments, molecular modeling on the basis of homology provides a valuable substitute for crystallographic data.

In principle, when comparing the sequences of distantly related modules, those which have vastly divergent functions but which still have the same protein fold,

conservation of residues reflects their importance in the protein fold. When aligning

sequences, amino acid residues which are essential in the formation of secondary

structures are likely to be conserved while those which form external loops to connect

structural motifs are likely to be variable in sequence and tolerant to deletions and

insertions (37, 38, 39). Predictions of secondary structures of homologous proteins

should reflect this similarity. The power of these sorts of predictions is seen in the fact

that they were used to correctly predicted the major structural features of kringles,

including β-sheets, β-turns, and external loops (38).

Though homology clearly plays a role with respect to protein structure, this is not

the case with protein function. The modules used to construct the regulatory proteases

have been shown to be present in numerous mosaic proteins with very different functions,

implying that structural homology does not necessarily lead to a similarity of function.

Regardless, structural homologies provide useful hints at possible functions that can be

tested experimentally.

1.6.2 Structural Similarity of the Vitamin K-Dependent Proteins

A great deal of structural homology is seen within the vitamin K-dependent

proteins that participate in the coagulation cascade and its regulation (see Figure 4) (16,

18, 49, 51). These proteins include factors VII, IX and X, as well as prothrombin, protein

C, and protein S. Each contains nine to twelve Gla residues in their amino terminal

region. Factors VII, IX and X, and protein C all have their Gla domains, containing

approximately 40 amino acid residues, followed by two EGF-like domains. These two

tandem repeats comprise approximately 50 amino acids each, and are followed by a

serine protease domain homologous to pancreatic trypsin. Protein S has four EGF-like domains, but lacks a serine protease domain (11).

Factors VII and IX, prothrombin, and protein S are all single chain proteins, while factor X and protein C are two-chain proteins with their light chain linked to the serine protease domain by a disulphide bridge. Factor X, protein C, and protein S all contain hydroxyaspartic acid, or hydroxyasparagine, in their EGF-like domains. With the exception of protein S, each requires cleavage of the polypeptide chain to activate the zymogen during the coagulation cascade. Protein S does not require minor proteolysis prior to its participation as a cofactor with activated protein C. (11, 12).

Figure 4: Domain Structures of the Vitamin K-Dependent Glycoproteins of Coagulation. The Gla residues in the N-terminal region are each indicated by a Y shape. In factors VII, IX and protein C the Gla domain is followed by two epidermal growth factor-like domains and the serine protease domain. In prothrombin the epidermal growth factor-like domains are replaced by two kringle domains. Protein S has four growth factor-like domains following the Gla domain but lacks a serine protease domain. Factors VII and IX, prothrombin and protein S are single-chain proteins, while factor X and protein C are two-chain proteins with a light chain linked to the heavy chain by a disulphide bond. Adapted from Davie et al., 1991.
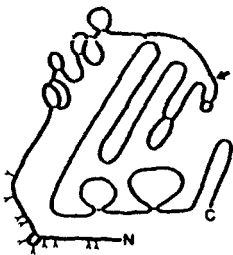
Factor VII
(Mr 50,000)
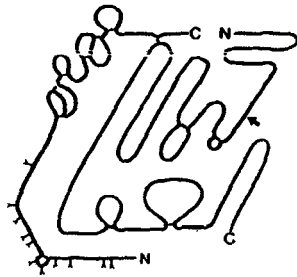
Factor X
(Mr 58,800)
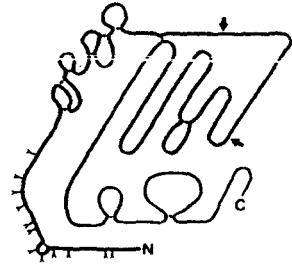
Factor IX
(Mr 56,000)
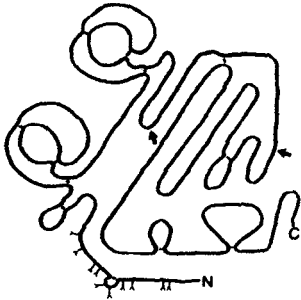
Prothrombin
(Mr 71,600)
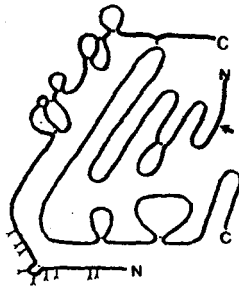
Protein C
(Mr 62,000)
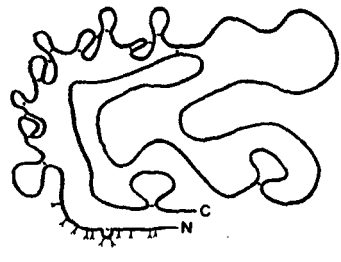
Protein S
(Mr 70,700)

1.6.3 Sequence Similarity of Ca^{2+}-Binding EGF-Like Domains

In addition to the structural similarity seen between the various vitamin K-dependent proteins, there are sequence similarities at the amino acid level (17, 34). Figure 5A shows an alignment of the EGF-1 domains of human coagulation factors VII, IX, X, with homologous residues indicated by shaded boxes. The first five amino acids of all four proteins are conserved. In only three of the latter 34 amino acids of the EGF-1 domain of factors VII, IX and X are there no conserved residues. The other 31 amino aids are conserved in at least two of the three proteins. These observations support the idea that the EGF-like modules are autonomous with respect to protein structure.

The sequence similarities of EGF-like domains can be further extended to those species other than man. Although the FVII EGF-1 sequence has been determined in only a few species, including the human, mouse, rabbit, bovine, canine, and Rhesus monkey, it can been seen that there is a high degree of homology at the amino acid level (22) (Figure 5B). Between the rabbit and human sequences, only six of 38 amino acids differ between the FVII EGF-1 domain and within the mouse and human sequences 11 of 38 amino acids differ. None of these differences occur at direct contact points between TF and FVII when in complex (1). Again it can be suggested that the conserved residues are those which are responsible for protein structure while the variable residues are responsible for the specific functional behavior of the individual protein.

Figure 5: Amino Acid Sequences of EGF-1 Domains. (A) Amino Acid

Sequence of the EGF-1 Domain of Human Factors IX, VII, X and Protein C.

The sequences are arranged so that the first cysteine residues are aligned.

Cysteine residues are shown in **bold**. Identical residues are shown in boxes with

░░░░░░. Factor IX and X sequences start at residue 47 while the factor VII

sequence starts at residue 46. Adapted from Chang et al., 1997. **(B) Amino Acid**

Sequence of the FVII EGF-1 Domain from Various Mammalian Species. The

amino acid sequences of the FVII EGF-1 domain from human, mouse, rabbit and

bovine are aligned. Specific nucleotide sequences are included for the human,

mouse and rabbit. The * indicates amino acid residues that are identical in all

four species. Between these species, only one of 18 bases differ at the N-terminus

and four of 18 bases differ at the C-terminus. These base pair changes are shown

in **bold.** The FVII EGF-1 domain spans residues 46 to 83. Adapted from

Idusogie et al., 1996.

(A)

```
                    1     2    1         2 3         3
Factor IX    DGDQCESNPCLNGGSCKDDINSYECWCPFGFEGKNCEL
Factor VII   DGDQCASSPCQNGGSCKDQLQSYICFCLPAFEGRNCET
Factor X     DGDQCETSPCQNQGKCKDGLGEYECTCLEGFEGKNCEL
```

(B)

```
        *   *   *   *   *   *   *       *   *   *   *       *       *           *
Human   D   G   D   Q   C   A   S   S   P   C   Q   N   G   G   S   C   K   D
          GATGGGGACCAGTGTGCCTCAAGTCCATGCCAGAATGGGGGGCTCCTGCAAGGAC
Mouse   D   G   D   Q   C   A   S   N   P   C   Q   N   V   G   T   C   Q   D
          GATGGGGACCAGTGTGCCTCGAATCCATGTCAGAACGTAGGTACCTGCCAGGAT
Rabbit  D   G   D   Q   C   A   S   N   P   C   Q   N   G   G   S   C   E   D
          GATGGGGATCAGTGTGCCTCCAACCCGTGCCAGAACGGAGGCTCCTGTGAGGAC
Bovine  D   G   D   Q   C   A   S   S   P   C   Q   N   G   G   S   C   E   D
```

```
            *   *       *   *   *           *   *   *   *   *   *
Human   Q   L   Q   S   Y   I   C   F   C   L   P   A   F   E   G   R   N   C
          CAGCTCCAGTCCTATATCTGCTTCTGCCTCCCTGCCTTCGAGGGCCGGAACTGT
Mouse   L   K   H   S   Y   V   C   F   C   L   L   D   F   E   G   R   N   C
          CATCTCAAGTCTTACHTCTGCTTCTGCCTCCTAGACTTTGAGGGTCGGAACTGT
Rabbit  Q   I   Q   S   Y   I   C   F   C   L   L   D   F   E   G   R   N   C
          CAAACTCAGTCCTACATCTGCTTCTGCCTGGCTGACTTCGAGGGTCGCAACTGT
Bovine  Q   L   R   S   Y   I   C   F   C   P   D   G   F   E   G   R   N   C
```

```
        *
Human   E   T
          GAGACG
Mouse   E   K
          GAGAAA
Rabbit  E   K
          GAGAAA
Bovine  E   T
```

1.7   Species Specificity of Tissue Factor

In 1984 Janson *et al.* published a study that showed variable clotting activities observed when plasma from a variety of species was combined with TF from various species (24). The values obtained for the homologous systems (i.e. human TF combined with human plasma or mouse TF combined with mouse plasma) were normalized to 100% thromboplastin activity. However, some very interesting observations were made when combining the plasma from species other than man with human TF. When plasma from rabbit was combined with human TF, a four-fold greater clotting activity was observed. Even more extraordinary, when mouse plasma was combined with human TF, a 13-fold greater clotting activity was seen. Conversely, the combination of plasma from horse and human TF produced a clotting activity of only one-third of that seen with the homologous human system. And the clotting activity of bovine plasma when combined with human TF was detected at less than 10% of that seen with plasma from human (24).

Although this study was not limited to the use of FVII, but rather employs plasma, which contains a complete complement of the clotting factors, it is well established that it is the FVIIa•TF complex that initiates the extrinsic pathway of coagulation (11). And formation of this complex requires the tight binding between the two proteins involved. Also well established, is the fact that the EGF-1 domain of FVII provides the majority of the binding area to TF in the FVIIa•TF complex (1). Taking these facts into account, the above studies suggest that there is a region of the FVII molecule, within species other than man, which generates its variable clotting activity when compared to wild-type

human FVII. Due to its key role in stabilizing the FVII•TF complex, this variation may

be due to differences in the EGF-1 domain.

1.8   Rationale and Objective of Current Study

The publication of Janson *et al.* (24) prompted the current study. We

hypothesized that by changing individual residues within the EGF-1 domain of wild-type

human FVII to the native residues found in other species, it might be possible to generate

a protein with increased TF binding. Specifically this was done making use of the two

species whose plasma, when combined with human TF, showed the greatest increase in

clotting activity. These were the mouse and rabbit species.

Using a variety of molecular biology techniques, chimeric proteins were

generated comprised of the wild-type human FVII molecule with its EGF-1 domain

exchanged for that from another species. In addition, FVII variants were created which

contain only single point mutations, based on differences between the species, within the

EGF-1, at the amino acid level. Since the EGF-1 domain of FVII has been demonstrated

to have the greatest single role in TF binding, it is possible that the phenomenon seen by

Janson *et al.* is due to this region. By creating the FVII variants using these techniques it

was ensured that the conserved residues necessary for protein folding were not changed

while those potentially responsible for the binding diversity would be altered. Ultimately

this could affect the TF binding properties of the FVII variants, possibly generating a

human FVII variant with a much higher affinity for human TF than wild-type human

FVII.

2.0 MATERIALS AND METHODS

2.1 Materials

2.1.1 Sources of Chemicals and Reagents

Chemicals were purchased from the following suppliers: Amersham Pharmacia

Biotech (Piccataway, NJ), T7 Sequencing kit; Boehringer Mannheim (GmbH, Germany),

CAT ELISA kit; Chromogenix-Instrumentation Laboratory (Milano, Italy), chromogenic

substrate S-2222; Clontech (Palo Alto, CA), Transformer Site-directed mutagenesis kit;

Enzyme Research Laboratories (South Bend, IN), plasma-derived human FVII, lot

#HFVII 1690; Fisher Scientific (Unionville, ON), Whatman #3 chromatography paper;

GibcoBRL (Canadian Life Technologies, Burlington, ON), Lipofectin reagent, cell

culture grade fetal calf serum, penicillin/streptomycin, cell culture grade 1x trypsin-

EDTA (0.05% trypsin, 0.53 M EDTA), TEMED, BSA, plasmid pUC19; Instrumentation

Laboratory Company (Lexington, MA), Hemoliance RecombiPlasTin recombinant

human tissue factor, lot # N0305392; Jackson Immuno Research Laboratories (Bio/Can

Scientific, Mississauga, ON), alkaline phosphatase-conjugated affinipure donkey α-sheep

IgG (H+L), alkaline phosphatase-conjugated streptavidin; MBI Fermentas (Burlington,

ON), T4 polynucleotide kinase, T4 DNA ligase, Eco91I (BstEII), AatII, NsiI, 6x loading

dye; New England Biolabs (Mississauga, ON), 1 kb DNA ladder; Pierce (Rockford, IL),

Micro BCA protein assay reagent kit; Promega Biotec (Unionville, ON), EcoRI, HindIII,

100 bp DNA ladder; λ/HindIII DNA ladder, RNaseA, dNTPs, X-gal, IPTG; Qiagen

Canada (Mississauga, ON), QIAprep Spin miniprep plasmid DNA isolation kit, QIAGEN

maxi plasmid purification kit, QIAEX II agarose gel extraction kit; Sigma Diagnostics

(St. Louis, MI), PNPP; Strategene (La Jolla, CA), *Pfu* polymerase, XL-1 Blue competent

cells.

DME/F12 medium and PBS were purchased from the Department of Pathology,

McMaster University. HEK 293 and BHK cells were purchased from the American

Tissue Type Culture Collection (Rockville, MD). All other reagents and chemicals not

mentioned above were of the highest quality available.

Rabbit FVII R152Q cDNA was previously cloned in the Clarke lab. NPP was

prepared by pooling citrated plasma from at least 20 healthy donors. The rabbit α-human

FVII and sheep α-human FVII antibodies were prepared by Myron Kulczycky. pCIS-

murine FVII cDNA was the generous gift of Dr. Francis Castellino (University of Notre

Dame). Recombinant TF apoprotein expressed in *E. coli* was a generous gift of

Genentech Inc. (36) (South San Francisco, CA).

2.1.2 Oligonucleotides

Oligonucleotides used for PCR, mutagenesis, and DNA sequencing, are listed in

Table 1. Each was synthesized at the Institute for Molecular Biology and Biotechnology,

McMaster University (Hamilton, ON). Primers were prepared desalted, and on a 40 nM

scale.

Table 1: Primers used for DNA Sequencing, Mutagenesis and PCR. All

primers used for sequencing, mutagenesis or PCR are listed by primer

identification number. A brief description of the each primer is given, including

its annealing position or the mutation that it introduces. For the mutagenesis and

PCR primers, bases in **bold** are those that have been changed and underlined

bases show the new restriction site generated.

PRIMER	OLIGONUCLEOTIDE SEQUENCE (5' to 3')	ANNEALING POSITION, MUTATION OR DESCRIPTION
SEQUENCING PRIMERS		
	ATT AAC CCT CAC TAA AGG GA	T3 promoter sequencing primer
AB6142	GGA GCT CAG TTG TGT GGG GG	Anneals hFVII at aa 670, forward sequencing
AB6143	CGT CCC GGG CAC CAC CAA	Anneals hFVII at aa 862, forward sequencing
AB6144	AGC TGC TGG ACC GTG GCG CC	Anneals hFVII at aa 1020, forward sequencing
AB16086	GAG GAG CAG TGC TCC TTC GAG G	Anneals hFVII at aa 216, forward sequencing through EGF-1 domain
AB16893	GGA CCT GCC ATG GAC ACT	Anneals hFVII at aa 666, reverse sequencing through EGF-1 domain
AB16894	CCT CCT TGC ACT CCC TCT	Anneals hFVII at aa 218, reverse sequencing
AB17598	TTC CTG GAG GAG CTG CGG C	Anneals hFVII at aa 170, forward sequencing through EGF-1 domain
AB18506	GAT CCG CCA CCA TGG TCT C	Anneals hFVII at aa 37, forward sequencing
MUTAGENESIS PRIMERS		
AB15657	GTG CCA CCT <u>GAT ATC</u> TAA GAA ACC	AatII→EcoRV unique site change, in pUC19 vector
AB15658	CTT ACA GTG AT<u>G GTG ACC</u> AGT GTG CCT C	BstEII site generation at 5' end of hFVII EGF-1
AB15659	CGG AAC TGT GAG <u>ATG CAT</u> AAG GAT GAC CAG C	NsiI site generation at 3' end of hFVII EGF-1
AB16220	GTG CCA CCT <u>GAC GTC</u> TAA GAA ACC	EcoRV→AatII unique site change, in pUC19 vector
AB16221	GC CGG AAC TGT GAG **AAA CAC** AAG GAT GAC CAG C	Correction of NsiI site in hFVII mouse EGF-1 chimera
AB16222	GGT CGC AAC TGT GAG **AAA CAC** AAG GAT GAC CAG C	Correction of NsiI site in hFVII rabbit EGF-1 chimera

PRIMER	OLIGONUCLEOTIDE SEQUENCE (5' to 3')	ANNEALING POSITION, MUTATION OR DESCRIPTION
MUTAGENESIS PRIMERS *continued*		
AB16596	TAC AGT GAT GG**G** GAC CAG TGT G	Correction of BstEII site in hFVII mouse EGF-1 chimera
AB16597	TAC AGT GAT GG**G** GA**T** CAG TGT GC	Correction of BstEII site in hFVII rabbit EGF-1 chimera
AB16864	G TGT GCC TCA **AA**C CCA TGC CAG AAT G	S53N hFVII point mutant
AB16865	G GGC TCC TGC **G**AG GAC CAG CTC	K62E hFVII point mutant
AB16856	GC TTC TGC CTC **G**CT GCC TTC GAG	P74A hFVII point mutant
AB16857	C TGC CTC CCT **GA**C TTC GAG GGC	A75D hFVII point mutant
AB16858	GC CGG AAG TGT GAG **AAA** CAC AAG GAT GAC C	T83K hFVII point mutant
AB19473 AB20663	GT CGG AAC TGT GAG **AAA** CAC AAG GAT GAC CAG C	Correction of NsiI site in hFVII mouse EGF-1 chimera
PCR PRIMERS		
AB15655	TAC AGT GAT <u>GGT GAC</u> CAG TGT GC	Forward mouse FVII EGF-1, 5' BstEII
AB15656	CTT **<u>ATG CAT</u>** CTC ACA GTT CCG ACC CTC	Forward mouse FVII EGF-1, 3' NsiI
AB15660	TAC AAT GAT <u>GGT GAC</u> CAG TGT GCC TCC	Forward rabbit FVII EGF-1, 5' BstEII
AB15661	TCT T**<u>AT GCA</u>** TCT CAC AGT TGC GAC CCT CG	Reverse rabbit FVII EGF-1, 3' NsiI

2.2   DNA Manipulations

2.2.1   Restriction Enzyme Digestions

Five to ten units of enzyme were used to digest 1 μg of plasmid DNA. DNA digestions were carried out under the conditions recommended by the manufacturer (with respect to buffer and temperature). Typically, DNA was transferred to a sterile microfuge tube, and reaction buffer, enzyme, and sterile ddH$_2$0 added, to a final volume of 20μL. The tubes was gently mixed, briefly centrifuged to collect the sample, and incubated 1 hour at 37°C. The enzyme reaction was terminated by heating at 65°C for 10 minutes.

The digested fragment was then isolated by either ethanol precipitation, or by gel-based analysis. To remove small fragments (<150 bp), the digested DNA was ethanol precipitated. 0.5 volumes of 1.29M NaAc, pH 5.2, and 2 volumes 95% EtOH were added to the DNA, the contents of the tube gently mixed, and incubated at -70°C for 30 minutes. The reaction tube was then centrifuged in a microcentrifuge for 15 minutes at maximum speed, at room temperature. The pellet was removed by aspiration, and washed once with 70% EtOH. After removal of the EtOH, the pellet was dried under vacuum in a SpeedVac concentrator (model SVG00H, Savant Instruments, Farmingdale, NY), resuspended in a suitable volume of ddH$_2$0, and ready for further manipulation. Gel-based isolation was preformed as later described (Sections 2.3.2 and 2.3.3).

2.2.2   Ligations of Plasmid DNA

All ligations were preformed at a 1:3 and 1:10 vector:insert DNA ratio. Digested vector DNA (10 ng) was transferred to a sterile microfuge tube, and a 3x or 10x molar

excess of insert DNA was added. 5 units of T4 DNA ligase, 2μL 10x ligation buffer, and ddH$_2$0 to a total volume of 20μL were then added. The tube was gently mixed, briefly centrifuged to collect the sample, and incubated for 2 hours at 16°C. The enzyme reaction was terminated by heating at 65°C for 10 minutes, and the DNA was ready to be transformed.

2.2.3   Site Directed Mutagenesis

Site directed mutagenesis was carried out using a Transformer site-directed mutagenesis kit, following the method of Deng and Nickoloff, 1992 (13). The included control mutagenesis reaction was carried out concurrently with all mutagenesis reactions. Initially, primers were phosphorylated by combining in a microfuge tube 10 units of T4 polynucleotide kinase, 2 μL of 10x T4 kinase buffer, 1 μg of primer, and ddH$_2$0 to a total volume of 20 μL. The tube was then vortexed to mix, centrifuged briefly, and incubated 1 hour at 37°C. The reaction was terminated by heating at 65°C for 10 minutes.

Primer was annealed to the DNA by combining in a microfuge tube 2 μL of 10x annealing buffer, 100 ng of plasmid DNA, 100 ng of unique site change selection primer, 100 ng of each mutagenic primer (one for each desired mutation), and ddH$_2$0 to a 20 μL total volume. The mixture was incubated for 3 minutes at 100°C, immediately chilled in an ice water bath for 5 minutes, and then briefly centrifuged to collect the sample.

The mutated DNA strand was synthesized by adding to the primer/plasmid annealing reaction 3 μL of 10x synthesis buffer, 1 μL of T4 DNA polymerase (2-4 units/μL), 1 μL of T4 DNA ligase (4-6 units/μL), and ddH$_2$O to a total volume of 30 μL.

The tube was mixed well, centrifuged briefly, and incubated 2 hours at 37°C. The DNA

was then ethanol precipitated, resuspended in 20 μL H_2O, and 2 μL 10x enzyme buffer

and 20 units restriction enzyme (able to cut the parental vector but not the mutated DNA)

added. The total volume was then adjusted to 30 μL with ddH_2O , and the tube incubated

2 hours at 37°C. The enzyme was inactivated by heating at 65°C for 10 minutes.

After digestion of the parental vector, the DNA pool was transformed into

BMH71-18 *mutS* cells, using a modified transformation protocol. Competent cells (100

μL) and 15 μL of the digested DNA pool were combined in a 15 mL snap-cap tube. The

tube was incubated on ice 20 minutes, and then heat shocked 1 minute at 42°C. 1 mL

room temperature LB was added, and the cells incubated 1 hour at 37°C, with shaking at

250 rpm, in order to facilitate protein expression. After incubation, an additional 4 mL of

LB + 100 μg/mL ampicillin was added, and the culture grown O/N at 37°C, with shaking

at 250 rpm, in an environmental shaker (model 3527, Lab-Line Instruments, Melrose

Park, IL).

Plasmid DNA was isolated from the O/N culture, using a QIAprep spin miniprep

kit. The DNA (5 μL) was then digested a second time with the selection enzyme against

the unmutated plasmid, following the same method as with the initial digestion. After

digestion, the DNA was transformed into XL-1 Blue cells using the same method as the

initial transformation. Following incubation for protein expression, serial dilutions of the

culture (100 μL total volume) were plated on LB plates, containing 100 μg/mL

ampicillin. 20 μL 2% X-gal and 10 μL 100 mM IPTG were added to the control

mutagenesis plates, in order to facilitate blue/white screening. Ideally, 70-90% of the control mutagenesis colonies should be blue after the final transformation. The plates were incubated O/N, inverted, at 37°C, for colony development. Colonies were randomly selected from the plates, and analyzed for incorporation of the desired mutation, by either restriction digest or manual sequencing.

2.2.4 Polymerase Chain Reaction

The following were combined in a sterile, 500 μL thin-walled PCR tube: 150 ng DNA, 10 μL *Pfu* buffer (contains $MgCl_2$), 0.8 μL dNTP (25 mM each), 0.5 μL of both sense and anti-sense primer (100 μM stock concentrations), and sterile ddH_2O, to a total volume of 98 μL. The reaction tube was placed in a programmable thermal cycler (model PTC-100, MJ Research, Watertown, MA), heated 5 minutes at 95°C, and the *Pfu* polymerase added.

Cycling was optimized to the following conditions (after the initial heating step): 45 seconds at 95°C, 45 seconds at 62°C, 1 minute at 72°C, with the process repeated 30x. After cycle completion, the reaction tube was incubated for an additional 10 minutes at 72°C, and then cooled to 4°C. Confirmation of the correct size fragment was accomplished by gel-based analysis.

2.3   Analysis of Nucleic Acids

2.3.1   Extraction and Purification of Plasmid DNA

2.3.1.1   Small Scale Extraction and Purification of DNA

For preliminary screening of mutagenesis clones for the incorporation of the desired mutation, plasmid DNA was prepared as follows: a 3 mL culture in

LB medium, supplemented with 100 μg/mL ampicillin, was inoculated from a single colony of transformed cells containing the desired plasmid gene of interest. The culture was grown by overnight incubation at 37°C, with shaking at 225 rpm, in an environmental shaker. 1.5 mL of the bacterial culture was centrifuged at room temperature for 1 minute at maximum speed in a microcentrifuge. The supernatant was removed by aspiration, and the pellet gently vortexed to resuspend the cells. 300 μL of TENS solution (100 mM NaOH, 0.5% SDS, in TE buffer) was added to lyse to cells, and the mixture inverted until clear. 150 μL of 3 M NaAc, pH 5.2, was added, and the tube vortexed gently to mix. The sample was centrifuged at room temperature for 10 minutes at maximum speed in a microcentrifuge. The supernatant was transferred to a fresh tube, and 900 μL of cold absolute ethanol was added to precipitate the plasmid DNA. The sample was centrifuged at room temperature for 2 minutes at maximum speed, and the supernatant again removed. The resultant pellet was washed with 70% EtOH, centrifuged at room temperature for 2 minutes at maximum speed. The supernatant was removed by aspiration, and the pellet dried under vacuum for 2 minutes in a SpeedVac unit. The pellet was resuspended 50 μL of TE buffer, pH 8.0, containing 50 μg/mL RNaseA, and was incubated at 55 °C for 15 minutes. To screen clones, 10 μl of the plasmid DNA was digested with the appropriate restriction enzyme, and run on an agarose gel.

For small-scale preparation of DNA which was required to be used for further molecular biology applications, a QIAprep Miniprep plasmid DNA

isolation kit was employed, adopting a modification of the method of Birnboim

and Doly (3). Each plasmid preparation would yield an average of 5-10 μg

DNA. All plasmid DNA was stored at -20°C.

2.3.1.2   Large Scale Extraction and Purification of DNA

Large scale purification of plasmid DNA was conducted using a

Qiagen Maxi plasmid purification kit, with the method of Birnboim and Doly (3).

The only change to the supplied protocol was the elimination of the second

centrifugation step before loading the bacterial cell lysate into the Qiagen-tip 500

column (step 8). Instead, the cell lysate was filtered through cheesecloth after the

initial centrifugation, and passed directly over the column. The DNA pellet was

resuspended in 200-400 μL TE buffer (10 mM Tris-Cl, pH 8.0; 1 mM EDTA),

depending on its size. Plasmid DNA was stored at –20 °C.

2.3.2   Gel Based Analysis of DNA

Agarose gels, 1% (weight:volume), were prepared in 1x TAE (89 mM Tris base,

89 mM acetic acid, 2 mM EDTA, pH 8.0), and heated in a microwave oven until the

agarose dissolved (approximately 2-3 minutes). The solution was cooled to 50–60°C,

and ethidium bromide added to a final concentration of 0.5 μg/mL. The liquefied gel was

added to a casting tray, and allowed to solidify at room temperature for 1 hour. DNA

samples and DNA marker standards, containing 1x loading dye, were loaded into the

wells and electrophoresed in 1x TAE at 80-100V. DNA bands were visualized on a

Fotodyne Foto/PrepI transilluminator (model C3-3500, New Berlin, WI). Digital

photographs were taken using a Kodak DC120 zoom digital camera, and developed with the supplied Kodak ds1D software.

2.3.3 Isolation of DNA from Agarose Gels

DNA was extracted from agarose gels using a Qiaex II Agarose Gel Extraction kit, following the supplied protocol. Typically 75% of the DNA was successfully isolated from the gel. Plasmid DNA was stored at -20°C until needed.

2.3.4 Quantification of DNA

Plasmid DNA was quantified using spectrophotometric absorbance at 260 nm. Plasmid DNA (5 μL) was diluted into 995 μL TE buffer and the A_{260nm} determined. The nucleic acid concentration was then calculated using Beer's law, and assuming that 1 A_{260nm} unit corresponded to 50 μg/mL of double-stranded DNA (44). When only an estimation of the DNA concentration was necessary, a sample of the plasmid DNA was electrophoresed under standard conditions (1% agarose gel, 1x TAE, 80-100V), and the quantity estimated by comparison by the relative band intensities of the sample against standard λ-HindIII DNA markers of known quantities.

2.3.5 Transformation of Competent Bacteria

2.3.5.1 Preparation of Chemically Competent Cells

A cell stock was streaked on an LB plate containing 1.5% agar (supplemented with 50 μg/mL tetracycline for BMH 71-18*mutS* cells, no antibiotic for XL1-Blue), and the plate incubated O/N at 37°C. A single colony was selected, and inoculated into a sterile tube containing 5 mL LB broth (supplemented with 50 μg/mL tetracycline for BMH 71-18*mutS* cells, no

antibiotic for XL1-Blue). The culture was incubated O/N at 37 °C with shaking at 225-250 rpm, in an environmental shaker. After O/N incubation, 1 mL of the saturated culture was transferred to a fresh, sterile 500- mL flask containing 100 mL of LB medium without antibiotic. The culture was incubated at 37 °C with shaking at 225-250 rpm, in an environmental shaker, until the OD_{600nm} was approximately 0.5 (typically 2.5-3 hours). The OD was frequently monitored once it reached 0.2 to avoid overgrowth. Once the culture had achieved the desired OD, the flask was chilled on ice for 20 minutes. The cells were collected by centrifugation at 1200 x g for 5 minutes in a Sorvall centrifuge (model RC5B Plus, Newton, CT), using a GSA rotor.

After resuspension in 10 mL ice-cold TSS solution (85% LB medium, 10% PEG (w/v; MW 8000), 5% DMSO (v/v), 50 mM $MgCl_2$ (pH 6.5), filter-sterilized), the cells were ready to be transformed. Chemically competent cells could be stored at 4°C for up to 6 hours, or at -70°C for long-term storage.

2.3.5.2   Chemical Transformation of XL-1 Blue Competent Cells

Competent cells were typically transformed directly after preparation. If the cells had been previously frozen, they were thawed on wet ice. DNA (typically 10 ng in a 1-3 µl volume) was combined with 100 µL of competent cells in a 1.5 mL microfuge tube. The tube was gently tapped to mix, incubated on ice for 30 minutes, and then heat shocked for 45 seconds at 37 °C. The tube was placed on ice an additional 2 minutes, followed by the addition of 900 µL of room temperature LB medium. Protein expression, including β-lactamase

ampicillin-resistance activity, occurred while incubating the tube an additional

hour at 37 °C with shaking at 225-250 rpm, in an environmental shaker. A 100

μL sub-sample of the transformed cells was then streaked onto an LB agar plate

containing the appropriate selection antibiotics for the transformed plasmid. The

plate was incubated inverted, O/N, at 37°C, for colony development.

2.3.6 DNA Sequencing

2.3.6.1 Manual Sequencing

The sequencing gel was prepared by combining 50 g of urea, 20 mL of

40% acrylamide/bis-acrylamide, 20 mL 5 x TBE, and 20 mL ddH$_2$0, and

dissolving the solution at room temperature with magnetic stirring. Once

dissolved, the solution was filtered under vacuum, and subsequently degassed

until no bubbles were present. 1 mL of 10% APS and 15 μL TEMED were

added, the solution gently swirled to mix, and immediately poured between glass

plates. The gel sandwich was clamped until polymerized, approximately one

hour.

Manual sequencing was carried out using a T7 DNA sequencing kit,

using the chain termination method. DNA samples were prepared by initially

denaturing the template DNA. In a microfuge tube, 20 μL of mini-prepared

plasmid DNA, 8 μL 1 M NaOH, 4 μL 2 mM EDTA, pH 8.0, and 8 μL sterile

ddH$_2$0, were combined. The tube was gently vortexed, centrifuged briefly, and

incubated 15 minutes at room temperature. 20 μL of 1.29 M NaAc, pH 5.0 was

added to neutralize the solution and 160 μL of absolute EtOH added to precipitate

the DNA. The tube was again mixed by gently vortexing and incubated at -70°C for 20 minutes. The sample was then microfuged 15 minutes at room temperature, and the supernatant removed. The pellet was washed once with 70% EtOH, spun for 5 minutes at room temperature, and the supernatant again removed. Any remaining traces of liquid were removed under vacuum, and the pellet resuspended in 10 μL sterile ddH$_2$0.

Annealing buffer (2 μL) and 1 μL of 1.0 μM sequencing primer were immediately added to the resuspended DNA pellet. The contents of the tube were mixed gently by vortexing, centrifuged briefly, and incubated for 5 minutes at 65 °C, immediately followed by incubation for 10 minutes at 37 °C, and 10 minutes at room temperature.

The enzyme sequencing premix was prepared as follows (where n is the number of samples to be sequenced): n μL sterile ddH$_2$0, $3n$ μL labeling mix, $2n$ μL diluted T7 DNA polymerase, and n μL S^{35}. The premix was kept on ice until ready to be used in the sequencing reactions. For each sample to be sequenced, 4 termination tubes were prepared (one for each of the nucleotides, labeled A, C, G and T), and 2.5 μL of the appropriate termination mix added. To conduct the actual sequencing reactions, 6 μL of premix was added to the annealed DNA/primer mixture, and the tube incubated 4 minutes at room temperature. The reaction was then split into the 4 termination tubes by pipeting 4.5 μL into each tube. The tubes were centrifuged briefly and incubated at 37 °C for 5 minutes.

Reactions were terminated by adding 5 μL of stop buffer and placing the samples

on ice. Samples were then run immediately or stored at −20 °C until they were

ready to be electrophoresed.

Before running, the sequencing gel was pre-electrophoresed on the

sequencing apparatus (model S2, Bethesda Research, Gaithersburg, MD) for 30

minutes, with 60 Watts constant power at 1600 V. Just prior to loading, the

samples were boiled for two minutes, and then 2 μL was loaded per well.

Sequencing gels were electrophoresed at 1600V with 60 Watts constant power.

Upon run completion, the gel was removed from the sequencing plate with a dry

sheet of Whatman paper, and dried 2 hours on a gel dryer (model 583, Bio-Rad,

Mississauga, ON). Once dry, the gel was exposed to X-ray film, and developed

after 36 to 48 hours.

2.3.6.2   Automated Sequencing

All automated sequencing was conducted at the Institute for Molecular

Biology and Biotechnology (MOBIX), at McMaster University, Hamilton,

Ontario.

2.4   Construction of the FVII EGF-1 Domain Exchange Mutants

2.4.1   Isolation of the EGF-1 Domain from Mouse and Rabbit cDNA

Initially, mouse and rabbit FVII EGF-1 domains were isolated from cDNA clones

using PCR as previously described. At the 5' and 3' ends, respectively, of the EGF-1

domain, BstEII and NsiI restriction enzyme sites were incorporated in order to facilitate

the cloning of the alternate EGF-1 domain into wild-type human FVII. PCR reactions

were carried out using the primers AB15655 and AB15656 for the mouse construct, and primers AB15660 and AB15661 for the rabbit construct, with pCIS-murineFVII and pCMV5rabbitFVIIR152Q cDNA, respectively.

2.4.2 Sub-cloning of Human FVII into pUC19

All mutagenesis was conducted in the cloning vector pUC19. Human FVII cDNA was initially excised from the expression vector pCMV5, and ligated into the multiple cloning site of the cloning vector pUC19, via the specific restriction sites EcoRI and HindIII.

2.4.3 Generation of BstEII/NsiI Restriction Sites within Human FVII

Using site directed mutagenesis, BstEII and NsiI sites were created at the 5' and 3' ends, respectively, of the EGF-1 domain of human FVII. Primers AB15658 and AB15659 were used to generate these sites, respectively. The unique site change incorporated into the parent vector, for the purpose of selection, was AatII→EcoRV, and employed primer AB15657. These sites were necessary to facilitate the subcloning of the EGF-1 domain from either mouse or rabbit into the human FVII molecule. Independent digestion of the resulting clones with BstEII and NsiI was conducted to confirm the generation of the desired sites.

2.4.4 Exchange of the FVII EGF-1 Domains

pUC19hFVII cDNA, containing the BstEII and NsiI sites, was digested with BstEII and NsiI to excise the EGF-1 domain, and subsequently ethanol precipitated to remove the EGF-1 fragment. The isolated EGF-1 domains from mouse and rabbit FVII were then ligated, independently, into wild-type human FVII via BstEII and NsiI sites.

The insertion of the alternate EGF-1 domain was confirmed by manually sequencing the new molecule from approximately 20 base pairs upstream of the EGF-1 domain to approximately 20 base pairs downstream of the EGF-1 domain.

2.4.5 Correction of the BstEII/NsiI Restriction Sites

A second round of site directed mutagenesis was conducted to correct the BstEII and NsiI restriction sites generated. For the mouse chimera, this involved primers AB16596 and AB19473, respectively. For the rabbit chimera, the primers used were AB16597 and AB16222. The unique site change in the parent vector for this round of mutagenesis was an EcoRV→AatII change, utilizing primer AB16220. These mutations were confirmed by the independent digestion the new DNA with the restriction enzymes BstEII and NsiI, with the desired clones being unable to be cut by either of these enzymes.

2.4.6 Cloning of the Human FVII Variant into pCMV5

Once the FVII EGF-1 domain exchange mutants were constructed, the FVII variant DNA was excised from the cloning vector via the EcoRI and HindIII sites of the multiple cloning site, and ligated into the multiple cloning site of the expression vector pCMV5. pCMV5hFVIImEGF-1 and pCMV5hFVIIrEGF-1 sequences were confirmed by automated sequencing of the entire FVII molecule.

2.5 Construction of the Human FVII Point Mutants

2.5.1 Sub-cloning of Human FVII into pUC19

All mutagenesis to create the point mutants was conducted in the cloning vector pUC19. Human FVII cDNA was excised from the expression vector pCMV5, and

ligated into the cloning vector pUC19, via the specific restriction sites EcoRI and HindIII.

2.5.2 Generation of the Point Mutations within Human FVII

Five human FVII point mutants with pUC19hFVII cDNA were created via site-directed mutagenesis, using the unique site elimination method, as previously described. The human FVII mutants generated were S53N, K62E, P74A, A75D and T83K, using the primers AB16864, AB16865, AB 16856, AB 16857 and 16858, respectively. The unique site change incorporated into the parent vector, for the purpose of selection, was AatII→EcoRV, and employed primer AB15657. The mutations were confirmed by manually sequencing of the changed amino acids only, with primer AB16086.

2.5.3 Cloning of the Human FVII Variant into pCMV5

Once the human FVII point mutants were constructed, DNA was excised from the cloning vector via the EcoRI and HindIII sites of the multiple cloning site, and ligated into the multiple cloning site of the expression vector pCMV5, via these same sites. The sequences of all human FVII point mutants were confirmed by automated sequencing through the full-length FVII molecule.

2.6 Expression of the Human FVII Variants

2.6.1 Maintenance of Cells in Growth Medium

Cells were initially grown in T75 screw-cap flasks (Corning), at 37°C in the presence of 5% CO_2. All cells were grown in complete growth medium (DME/F12 supplemented with 10% FCS, 1% P/S, and 100 ng/mL vitamin K). Once cells reached approximately 90% confluence, they were split by initially aspirating off the old media

then washing the cells twice with PBS. A 1.5 mL volume of trypsin-EDTA was added to

remove the adherent cells from the flask wall and the cells were incubated at RT under

sterile conditions for approximately 5 minutes. Cells were then resuspended in complete

growth medium, and a portion of the resuspended cell solution was added to a new flask

containing 20 mL of fresh complete growth medium.

2.6.2   Transfection of Cells Using Liposome-Mediated Transfer

Transfection was performed in 6 x 35mm well plates (Falcon). A monolayer

culture of cells was grown in 3 mL of complete growth medium to a confluency of

approximately 70-80%. Two wells were simultaneously transfected for each construct,

and the resultant tissue culture media was pooled after transfection for analysis.

For each transfection, 200 μL of transfection media (DME/F12 supplemented

with 100 ng/mL vitamin K) was added to 2 x 1.5 mL sterile Eppendorf tubes. To one

tube, 10 μL of Lipofectin reagent was added. To the second tube, 2 μg of the desired

FVII cDNA, in the expression vector pCMV5, plus 160 ng of the transfection efficiency

control plasmid, pCMV-CAT, were added. This constituted a 1:10 molar transfection

ratio of control plasmid:rFVII variant. The contents of each tube were then combined,

mixed gently by inversion, and incubated for 15 minutes at room temperature under

sterile conditions. After the incubation, the DNA-Lipofectin complex was added to a

5mL sterile polystyrene tube containing 3.6 mL transfection media.

Cells were washed once with transfection media, and 2 mL of the DNA-

Lipofectin complex was added to each of the 2 dishes of cells. The cells were then

placed in a 37°C incubator in the presence of 5% CO_2. After 6 hours, the DNA-

Lipofectin mixture was removed by aspiration, and replaced with 2 mL complete growth medium. After an additional 40-44 hours, the complete growth media was replaced with a modified complete growth medium (BIT-GM). This media was the same as the initial growth medium, with the FCS substituted by a combination of transferrin, insulin, and albumin. The complete growth media was removed by aspiration, and the cells washed 2x with DME/F12, to ensure the complete removal of all FCS. A 3 mL volume of BIT-GM was then added to each well. Cells were incubated a further 48 hours at 37°C in the presence of 5% CO_2.

2.6.3 Harvesting of the Culture Media

Ninety-six hours post transfection, the conditioned culture media was harvested. The media from each of the 2 dishes transfected with the same DNA was combined in a 15 mL polystyrene tube. The media was centrifuged at 3,000 rpm for 10 minutes at room temperature in a tabletop centrifuge (Sorvall model RT6000B, Newtown, CT), in order to remove all traces of cell debris. The resultant supernatant was placed in a fresh 15 mL tube, and stored at -70°C until needed.

Cell extracts were prepared using lysis buffer from the commercial CAT ELISA kit. After the conditioned media was harvested, cells were washed 3x with cold PBS, ensuring all trace of PBS were removed after the final wash. A 500 μL volume of lysis buffer was added to each 35mm dish, and the cells let stand 30 minutes at room temperature. The cell extract was then transferred to a microfuge tube and centrifuged at maximum speed for 10 minutes at 4°C, to remove any cellular debris. The supernatant was transferred to a fresh tube, and either used immediately or stored at -70°C.

2.7 Analysis and Characterization of the Recombinant FVII Variants

2.7.1 Transfection Efficiency

The determination of transfection efficiency was a 2-step process conducted on the cell lysate of transfected cells.

2.7.1.1 Total Protein Levels in Cell Lysate of Transfected Cells

The total protein in the cell lysate of transfected cells was determined using a commercial BCA protein assay kit, following the supplied protocol. A 100 μL volume of cell extract (diluted 100x in ddH$_2$O) or BCA protein standard was added to a microtiter plate well, in triplicate. The working reagent was prepared as follows: 25 parts Reagent MA (containing sodium carbonate, sodium bicarbonate and sodium tartrate in 0.2 N NaOH), 24 parts Reagent MB (containing 4% bicinchoninic acid in H$_2$0), and 1 part Reagent MC (containing 4% cupric sulfate, pentahydrate in H$_2$0). 100 μL of the working reagent was then added to each well, the plate mixed well, covered, at incubated 2 hours at 37°C. After incubation, the plate was cooled to room temperature and the absorbance read at 562 nm in an automated microtiter plate reader (model EL808, Bio-Tek Instruments, Winooski, VT), utilizing the supplied KC4 Kineticalc software, version 2.0. A standard curve was developed using the BSA standards, and the protein concentration of the cell lysate determined for each unknown sample.

2.7.1.2 CAT Concentration in Cell Lysate of Transfected Cells

CAT levels in the cell lysate were determined using a commercially available CAT ELISA kit, in order to normalize the total FVII antigen levels in

the transfection medium for transfection efficiency. The assay was carried out following the supplied protocol. A 200 μL volume of cell lysate (diluted 75x in sample buffer) or CAT standard was added to a microtiter plate (MTP) module, coated with anti-CAT antibody, in triplicate. The plate was covered and incubated 1 hour at 37°C. The wells were washed 5x with washing buffer (solution 6), and 200 μL of anti-CAT-DIG antibody (solution 2a) added to each MTP module. The plate was again incubated 1 hour at 37°C, and following incubation, washed 5x with washing buffer. A 200 μL volume of anti-DIG-POD antibody (solution 3a) was then added to each MTP module, and the plate incubated 1 hour at 37°C. After washing 5x with washing buffer, 200 μL of POD substrate (solution 4) was added to each well, and the plate incubated, with shaking, until color development (typically 15-30 minutes). Sample absorbance was measured at 405 nm (490 nm reference wavelength) in a microtiter plate reader. A standard curve was generated using the CAT standards, and the CAT concentration in the unknown samples determined from this linear calibration curve.

2.7.2 Total FVII Antigen Concentration in Tissue Culture Media

Approximately 500 ng of rabbit α–human FVII antibody, in CACB, pH 9.6, was coated per well, in a 96-well plate. After overnight incubation at 4°C, the plate was washed 2x with TBS-T buffer. Non-specific binding was blocked by the addition of 200 μL TBS-T with BSA (1 mg/mL), and incubation for 2 hours at room temperature. The plate was then washed 2x with TBS-T, followed by the addition of either plasma-derived

FVII standards to develop the standard curve, or tissue culture samples containing an unknown quantity of rFVII. All dilutions of the samples were done in DME/F12. The plate was incubated a further 2 hours at room temperature.

The plate was then washed 4x with TBS-T buffer, and 100 μL of biotinylated rabbit α-human FVII antibody (0.5 μg/mL), in TBS-T with BSA, was added to each well. Incubation was carried out for 1 hour at room temperature. The plate was again washed 4x with TBS-T buffer, followed by the addition of 100 μL streptavidin-AP (1:2000 diluted, 1 mg/mL stock), and incubation for 1 hour at room temperature. The plate was then washed a final 4x with TBS-T, and 100 μL PNPP (1mg/mL) in diethanolamine buffer was added to each well.

The plate was incubated in darkness until color development (approximately 45 minutes), and then scanned at 405 nm in a microtiter plate reader. A standard curve was generated from the FVII standards, and FVII antigen concentrations for the unknown samples determined from this curve. FVII levels were also normalized for transfection efficiency, by comparison to CAT levels in the cell extract.

2.7.3 Biological Activity

2.7.3.1 Prothrombin Time

100 μL of tissue culture media, containing 15 ng rFVII/mL, and diluted in pCMV5 mock-transfected cell culture media, was combined with 100 μL FVII-depleted plasma, and warmed to 37°C for exactly 2.5 minutes. 200 μL of commercial recombinant TF warmed to 37°C for between 2 and 10 minutes, was added, and the time for clot formation determined using a fibrin timer (Coa

SYSTEM analyzer model, LAbor Instruments, Hamburg, W. Germany). Each sample was run in triplicate.

A standard curve was generated in the same manner, with the rFVII sample being replaced by serial dilutions of NPP (2x to 128x diluted). FVII clotting activity (mU/mL) was plotted against PT (seconds), on a log-log scale. FVII clotting activity of the rFVII variants was determined by reference to the calibration curve, taking into account the dilution factor of the test samples.

2.7.3.2   Amidolytic Activity

A concentration of 10 ng/mL rFVII, diluted to 100 μL in tissue culture media, was used in each assay. A 25 μL volume of 25 mM $CaCl_2$, and 50 μL FX (18 μg/mL stock in 0.05 M Tris-Cl, pH 8.0, 0.15 M NaCl, 1 mg/mL BSA), were combined in a 1.5 mL Eppendorf tube, and incubated 1-2 minutes at 37°C. 50 μL commercial recombinant TF was added, each tube vortexed gently, and the reaction allowed to continue for exactly 3 minutes at 37°C. EDTA (0.3 M) was added to a final concentration of 0.03 M to terminate the reaction. After vortexing, each tube was incubated on ice until ready to proceed to the second stage (typically 10-20 minutes).

In a 1.5 mL cuvette, 516 μL buffer (0.05 M Tris-Cl, pH 8.0, 0.15 M NaCl) and 21.5 μL of 4mM S-2222 were combined. A 62.5 μL volume of the reaction mixture from the first stage was added to the cuvette. The contents were mixed by inversion, and the rate of reaction determined at 405 nm, at 15 second

intervals, for 2 minutes (45). The $\Delta A405nm$/minute was determined from the

initial slope of the curve (typically the first 4 readings).

2.7.4 Direct TF Binding

Direct TF binding by the rFVII variants was determined using a modified

"TRAP" ELISA (47). Approximately 20 ng of TF apoprotein, in CACB, was coated per

well, in a 96-well plate. After overnight incubation at 4°C, the plate was washed 2x with

0.9% NaCl, followed by a single wash with TBS-T buffer containing 10 mM Ca^{2+}. Non-

specific binding was blocked by the addition of 200 µL TBS-T buffer containing 10 mM

Ca^{2+} and 1 mg/mL BSA, and incubation 1.5 hours at 37°C. The plate was then washed

2x with TBS-T buffer containing 10 mM Ca^{2+}, followed by the addition of rFVII in tissue

culture media, at a concentration of 20 ng/mL. All dilutions of the samples were done in

mock-transfected media. The plate was incubated for an additional 1.5 hours at 37°C.

The plate was then washed 2x with TBS-T buffer containing 10 mM Ca^{2+}, and

100 µL of sheep α-hFVII (1:10,000 dilution, 10 mg/mL stock), in TBS-T with 10 mM

Ca^{2+} and 1 mg/mL BSA, was added to each well. The plate was incubated for 1 hour at

37 °C. The plate was washed 4x with TBS-T buffer containing 10 mM Ca^{2+}, followed by

the addition of 100 µL AP-conjugated donkey α–sheep IgG (1 mg/mL stock, 1:10,000

diluted), and incubation for 1 hour at 37 °C. The plate was washed a final 4x with TBS-T

buffer containing 10 mM Ca^{2+}, and 100 µL PNPP (1 mg/mL) in diethanolamine buffer

was added to each well. The plate was incubated in darkness at room temperature until

color development (typically 16 hours), and then scanned at 405 nm in an automated

microtiter plate reader.

A standard curve was initially constructed to determine the linear range of the assay. Plasma derived human FVII, at concentrations of 1-50 ng/mL, was diluted in mock-transfected tissue culture media, and substituted for the rFVII in the above assay. No other changes were made.

2.7.5 Computer Modeling of FVII Variant Structures

Computer predictions of the structures of the FVII variants constructed were made using the Swiss-Pdb Viewer program, version 3.51, available from Glaxo Wellcome Experimental Research (http://www.expasy.ch/spdbv). Coordinates for the FVIIa•TF complex are from the Protein Data Base, file 1DAN.pdb.

3.0   RESULTS

3.1   Construction of the FVII EGF-1 Domain Exchange Chimeras

A complete list of the FVII variants constructed is shown in Appendix A.

3.1.1   Isolation of the EGF-1 Domain from Mouse and Rabbit cDNA

The mouse and rabbit FVII EGF-1 domains, incorporating the additional BstEII

and NsiI sites at the 5' and 3' ends, respectively, were successfully isolated from cDNA

clones using PCR. Isolation of the EGF-1 domain was confirmed by gel based analysis,

which revealed the desired 127 bp fragment (Figure 6)

3.1.2   Generation of BstEII/NsiI Restriction Sites within Human FVII

BstEII and NsiI sites were created within the human FVII molecule in the cloning

vector pUC19. This mutagenesis yielded approximately 300 colonies after the final

transformation. Eighteen colonies were selected to check for the desired mutation, and

initially digested with BstEII. Twelve of the 18 colonies incorporated the BstEII

mutation, and these clones were then digested with NsiI to see if the second mutation had

also been incorporated. Each of the 12 colonies was successfully digested with NsiI.

One of the 12 colonies was then chosen, at random, for continuing experimentation. The

control mutagenesis was conducted simultaneously, with a success rate of approximately

80%, as determined by blue-white screening.

3.1.3   Exchange of the EGF-1 Domains

The mouse and rabbit EGF-1 domains were ligated, independently, into the

human FVII molecule, and the resultant DNA transformed into XL-I Blue cells. In both

cases, approximately 300 colonies resulted on the transformation plates, with no colonies on the control (vector only) ligation plate. Three colonies were randomly chosen from each of the ligations, and were manually sequenced through the region encoding the EGF-1 domain. Each had the desired sequence and one clone of each chimera was selected for further manipulation.

3.1.4   Correction of the BstEII/NsiI Restriction Sites

With the rabbit chimera, this round of mutagenesis yielded approximately 400 colonies after the final transformation. Eighteen colonies were selected to check for the desired mutation, and initially digested with BstEII. Fifteen of the 18 colonies had the BstEII site eliminated, and these clones were subsequently digested with NsiI to see if the second site had also been eliminated. Fourteen of the 15 colonies had the NsiI site successfully eliminated. One of the 12 colonies was then chosen, at random, to continue with.

With the mouse chimera, approximately 100 colonies were obtained after this round of mutagenesis. Eighteen colonies were selected to check for the desired mutation, and initially digested with BstEII. Thirteen of the 18 colonies had the BstEII site eliminated. Of these clones, none had the NsiI site successfully eliminated. Eighteen additional clones were chosen, and 12 of the 18 had the BstEII site eliminated. Of these 12 clones, none had the NsiI site eliminated. When the mutagenesis was repeated, attempting only to change the NsiI site, again it was unsuccessful. Thirty-six colonies were chosen, and none had the NsiI site eliminated. After the second attempt at the

mutagenesis, it was decided to leave the mouse chimera as it was, and continue working with the chimera with the restriction sites still in place.

During all attempts at the second round of mutagenesis, the control mutagenesis was conducted simultaneously. Its success rate was between 70 and 80%, as determined by blue-white screening.

3.1.5 Cloning of the Chimeric FVII into pCMV5

The FVII chimeras were each ligated into the expression vector pCMV5, and the resultant plasmid transformed into XL-I Blue cells. The transformation of each chimera yielded approximately 250 colonies, with no colonies on the control (vector only) ligation plate. Six colonies were randomly chosen from each of the ligations and were simultaneously digested with EcoRI and HindIII. Each of the colonies yielded the desired 1400 and 4900 base pair fragments (Figure 7).

One clone of each of the chimeras was then randomly chosen and sequenced by automated sequencing through the entire length of the FVII molecule. With each chimera, the desired FVII sequence was present. Four silent mutations were found within the FVII molecule. At amino acid 148 the nucleotide sequence changed from AAA→AAG, at residue 151 the nucleotide sequence was changed from GCC→GGG, at amino acid 208 the nucleotide sequence was changed from CTG→CTC, and the nucleotide sequence was changed from GGC→GGG at residue 209. None of these substitutions coded for an alternative amino acid, as the codons AAA and AAG both code for a lysine, GGC and GGG both code for a glycine residue, and the codons CTG and CTC both code for a leucine residue.

Figure 6: PCR Amplification of the FVII EGF-1 Domain from Mouse and Rabbit. The 127 base pair EGF-1 domain was isolated from mouse and rabbit FVII cDNA via PCR, and confirmed by agarose gel-based analysis of the product. Lane 1 shows the PCR product from the mouse EGF-1 domain amplification with lane 2 a positive control for the mouse PCR. Lane 3 shows the PCR product from the rabbit EGF-1 domain amplification with lane 4 a positive control for the rabbit PCR. The desired 127 bp residue is indicated with an arrow. To the right of the rabbit control is the negative PCR control, in which no DNA was added to the reaction. The far right lane contains the 100 bp DNA ladder used as a marker, with the relevant bands indicated.
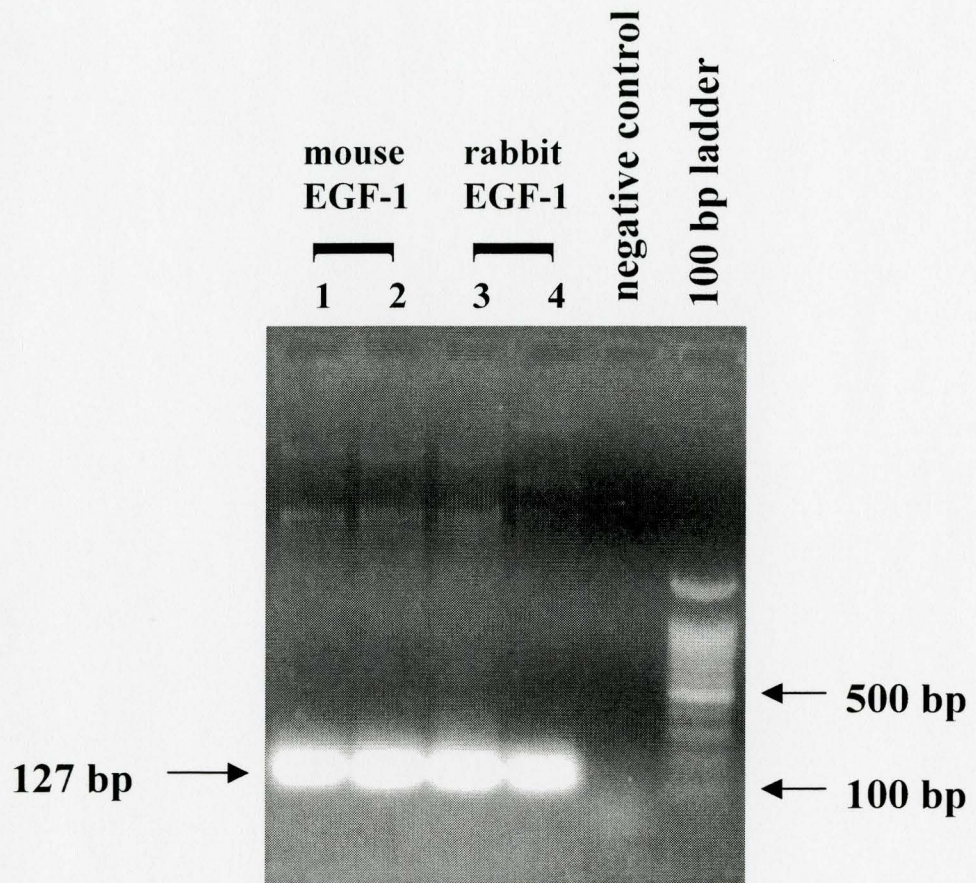
Figure 7: EcoRI/HindIII Digest of the FVII EGF-1 Chimeras in pCMV5.

This gel shows the fragments generated by EcoRI/HindII digestion of the mouse

chimera "M" and the corrected rabbit chimera "R CORR" after ligation into the

expression vector pCMV5. Successful ligation yielded 2 fragments. The pCMV5

vector is 4900 bp and the FVII molecule is 1400 bp. Lanes 1 to 5 show the

digestion of 5 clones of the mouse chimera and lanes 6 to 10 show the digestion

of five clones of the corrected rabbit chimera. With each the desired bands are

indicated with arrows. A 1 kb ladder is shown in the far left lane, with the

relevant bands labeled.
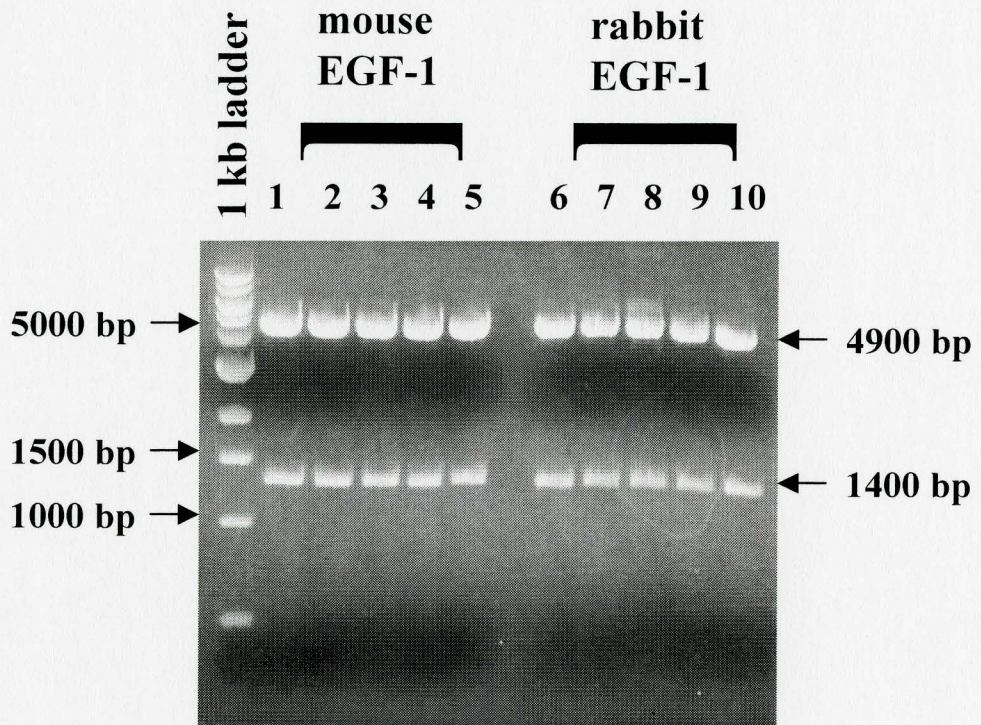
3.2 Construction of the Human FVII Point Mutants

A summary of the FVII point mutants constructed can be seen in Appendix A.

3.2.1 Generation of the Point Mutations within Human FVII

The five point mutants were created independently within the human FVII molecule, in the cloning vector pUC19. Each mutagenesis reaction yielded between 500 and 800 colonies after the final transformation. Eight colonies of each point mutant were randomly chosen and digested with EcoRV, to check for the incorporation of the selection site and the correct plasmid size of approximately 6400 base pairs. Typically two or three (sometimes more) colonies were of the correct size and had incorporated the EcoRV selection site (Figure 8). During this mutagenesis, the control mutagenesis was conducted simultaneously. Its success rate was approximately 70%, as determined by blue-white screening.

Clones with the selection site successfully incorporated were manually sequenced through the mutated area to confirm the desired mutations to the FVII EGF-1 domain. One clone of each point mutant was chosen to continue with.

3.2.2 Cloning of the Human FVII Point Mutants into pCMV5

The human FVII point mutants were each ligated into the expression vector pCMV5, and the resultant DNA transformed into XL-I Blue cells. Each chimera yielded approximately 200 colonies on the transformation plates, with no colonies on the control (vector only) ligation plate. Six colonies were randomly chosen from each of the ligations and digested with EcoRI and HindIII. Each of the colonies yielded the desired 1400 and 4900 base pair fragments.

One of each of the point mutants was randomly selected and sequenced by automated sequencing through the full-length of the FVII molecule. With each point mutant, the entire FVII sequence was intact and the desired mutation incorporated. Four additional point mutations were found within the FVII molecule, each of which generated only a silent mutation not coding for any changes in amino acid residues. These mutations are the same as those described with the FVII EGF-1 domain chimeras, in section 3.1.5.

Figure 8: EcoRV Digest of Human FVII Point Mutation Clones in pUC19.

This gel shows the fragments generated by EcoRV digest of the human FVII point

mutants in the cloning vector pUC19. Successful incorporation of the mutagenic

selection site will yield DNA that is cut by this enzyme, generating a single

fragment 4100 bp in size, indicated by an arrow. For each of the five point

mutants constructed, 3 digested clones are shown. Each lane is labeled 1 through

3, underneath of its corresponding mutant name. Successful incorporation of the

mutation, as indicated by a 4100 bp fragment, is seen in lane 1 with S53N, lane 2

with K62E, lane 3 with P74A, and lane 3 with T83K. No 4100 bp bands are seen

for the A75D mutation on this gel, though the desired band was found during the

screening of additional clones. Uncut pUC19 FVII DNA was used as a control

and is shown in the far left lane of the gel. Adjacent to the negative control is the

1 kb ladder. In the far right lane λ HindII DNA was run as an additional marker.
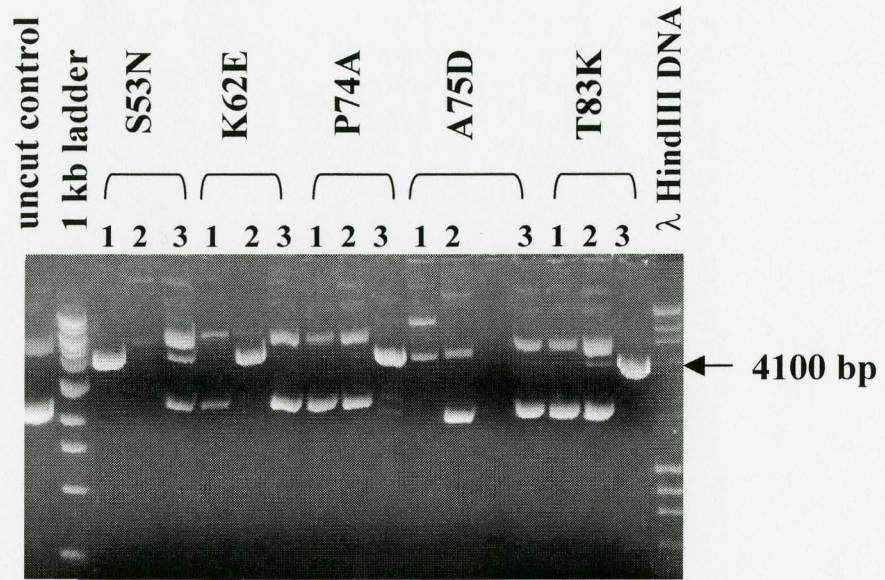
3.3   Transfection Efficiency

Transfection efficiency was determined independently for each of the three transfections conducted. Results are shown in Table 2. For the first transfection, the greatest efficiency was seen with the mouse chimera, designated as 100%. The next best transfection efficiencies were seen for the human variant "H" and the CAT-only constructs, at 79% and 60%, respectively. All other constructs were transfected with efficiencies ranging from 26% to 51%.

In the second transfection, the greatest transfection efficiency was seen with wild-type human FVII. In general, the transfection efficiencies seen in this transfection were much greater than those seen with the first transfection. The other constructs transfected had efficiencies in the range of 51% to 85%. The exception to this was the R79Q mutant, which was transfected at only a 17% efficiency (in the first transfection this construct had a 47% efficiency).

In the third transfection, the range of efficiencies was the most extensive. Both the uncorrected rabbit chimera "R" and the T83K point mutant were transfected at 100% efficiency. Wild-type human FVII and point mutants S53N and T83K also had efficiencies greater than 90%. The human variant "H", the mouse chimera, the uncorrected rabbit chimera "R" and the point mutant A75D were all transfected with efficiencies above 50%, at 62%, 53%, 79% and 70%, respectively. The CAT-only construct and point mutant K62E were transfected between 30% and 40%, while the lowest efficiency was again seen with R79Q, at only 12%.

Table 2: Transfection Efficiency. The efficiency of transfection, as a percentage, is shown for each of the transfections conducted. A description of each of the FVII variants listed can be seen in Appendix A. For each independent transfection, efficiency was determined by dividing the amount of CAT enzyme present in the transfected cell extract by the total protein content of the cell extract. The highest relative value was then designated as 100% efficiency, and all other values normalized with respect to it. The control media has an efficiency of 0 as the pCMV-CAT vector was not co-transfected.

FVII	Transfection Efficiency (%)		
Variant	Transfection 1	Transfection 2	Transfection 3
WT	51	100	98
R79Q	47	17	12
CONT	0	0	0
CAT	60	61	32
H	79	69	62
M	100	51	53
R	40	63	100
R CORR	33	58	79
53	39	56	91
62	26	57	42
74	34	81	98
75	46	60	70
83	39	85	100

3.4   Total FVII Antigen Concentration in Tissue Culture Media

A standard curve was initially developed, and used as a reference to determine the total antigen levels of the recombinant FVII variants in the tissue culture media (Figure 9). The linear range of the assay was determined as lying between 2 and 50 ng/mL FVII, and it was ensured that antigen levels used, after dilution, fell within these boundaries.

Three independent transfections were conducted, producing varying levels of recombinant FVII protein. Because there was no detectable FVII in the culture media from the mouse chimera transfections during preliminary experiments, the mouse chimera was transfected in duplicate or triplicate during each of the final transfections. All transfections of the mouse chimera yielded the same result (no detectable FVII).

In the first transfection, FVII levels produced ranged from 20 ng/mL to 76 ng/mL (Figure 10A). There was no detectable FVII found with the negative control, the CAT-only transfected control, and the mouse chimera. The greatest FVII levels seen were for the human variant "H" and the wild-type human FVII transfections, at 76 ± 7 ng/mL and 68 ± 3 ng/mL, respectively. The uncorrected rabbit chimera was secreted into the media at 41 ± 4 ng/mL, while all other constructs showed FVII levels between 20 and 35 ng/mL ± 2-5 ng/mL.

Once normalized for transfection efficiency, the FVII levels ranged from 45 to 132 ng/mL. After normalization, the lowest detectable levels were seen with R79Q and the point mutant A75D, at 45 ± 3 ng/mL and 46 ±6 ng/mL,

respectively. With the exception of wild-type human FVII, which after

normalization had a FVII concentration of 132 ± 6 ng/mL, all other constructs had

FVII concentrations normalized to 60 to 100 ng/mL.

In the second transfection, FVII levels ranged from 20 ng/mL to 73 ng/mL

(Figure 10B). Again, no detectable FVII was seen in the negative control

transfection, the CAT-only transfection, and the mouse chimera transfection. The

highest FVII level seen was for the T83K point mutant, at 73 ± 7 ng/mL. The

human variant "H" and the point mutant S53N had FVII levels of 44 ± 3 ng/mL

and 46 ± 3 ng/mL, respectively. All other constructs showed FVII levels between

25 ng/mL and 35 ng/mL, with the exception of R79Q, which had an antigen

concentration of only 20 ± 2 ng/mL.

Once normalized for transfection efficiency, the FVII levels ranged from

35 to 113 ng/mL. After normalization, the lowest detectable levels were still seen

with wild-type human FVII, as it was transfected with 100% efficiency. The

corrected rabbit chimera "R CORR", and point mutants P74A and A57D all had

FVII concentrations normalized to approximately 40 ng/mL. Levels in the human

variant "H", the uncorrected rabbit chimera "R", and point mutant K62E were

slightly higher, between 52 and 64 ng/mL. Point mutants S53N and T83K had

their antigen concentrations normalized to between 81 and 86 ng/mL. The

greatest normalized FVII concentration was seen with R79Q, at 113 ± 12 ng/mL.

In the third transfection, FVII levels ranged from 20 ng/mL to 60 ng/mL

(Figure 10C). Again, no detectable FVII was seen in the negative control

transfection, the CAT-only transfection, and the mouse chimera transfection. The highest FVII level seen was for the human variant "H", at 60 ± 8 ng/mL. Wild-type human FVII had 38 ± 4 ng/mL FVII, while other constructs showed FVII levels between 20 ng/mL and 33 ng/mL. The lowest FVII levels were seen with R79Q and the point mutant A75D, both at 20 ± 2 ng/mL.

Once normalized for transfection efficiency, the FVII levels ranged from 23 to 158 ng/mL. After normalization, the lowest FVII level was seen with the point mutant P73A, at 23 ± 3 ng/mL. With the exception of K62E, all of the point mutants, as well as wild-type human FVII and both the rabbit chimeras "R" and "R CORR", all maintained FVII levels below 40 ng/mL. Point mutant K62E was normalized to 59 ± 6 ng/mL FVII and the human variant "H" was normalized to 98 ± 13 ng/mL. R79Q had the greatest FVII level after normalization, at 158 ± 7 ng/mL.

Figure 9: Standard Curve for the Total FVII Antigen ELISA. The standard

curve for the FVII antigen ELISA was developed using plasma derived human

FVII. The linear range of the assay is between 2 and 50 ng/mL FVII.
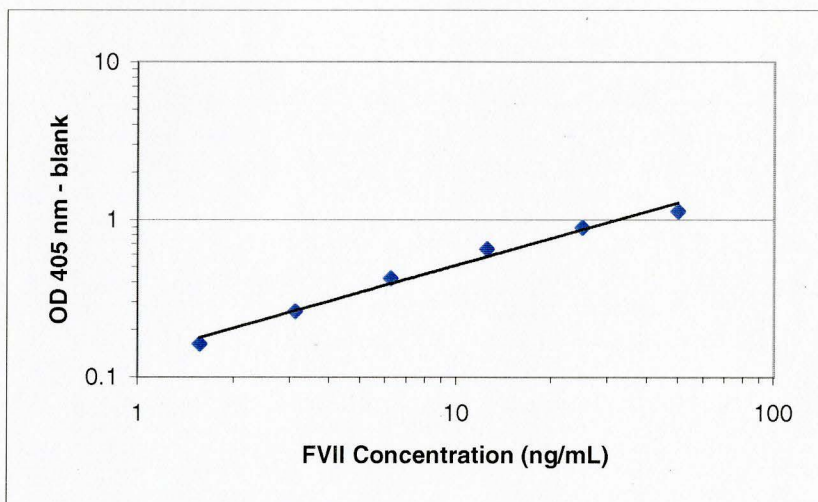
Figure 10: FVII Antigen Secreted by 293 Cells Transfected with rFVII
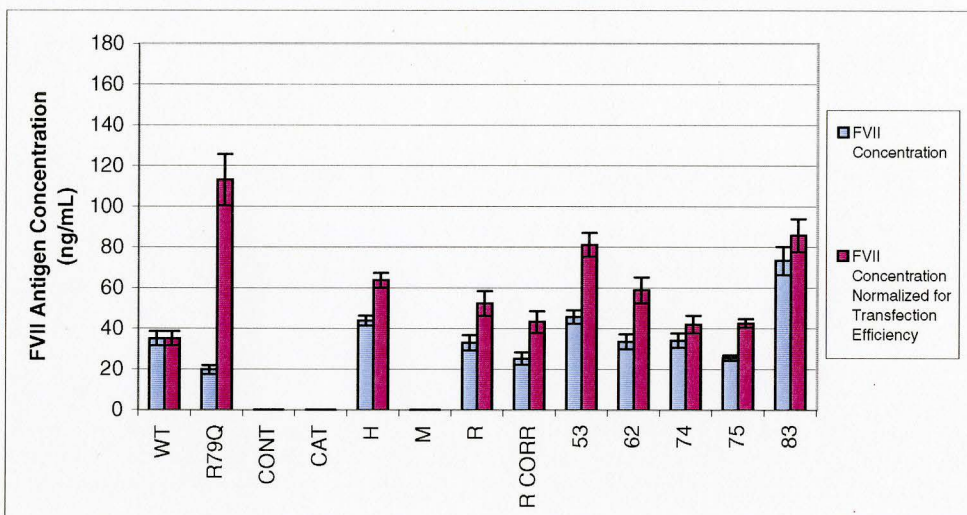
Variants. Panels A-C show the FVII concentration in the conditioned culture

media from transfection experiments 1-3, respectively. Blue bars show actual

levels of FVII antigen detected in the conditioned culture media. Red bars show

the FVII antigen levels after correction for transfection efficiency. Error shown is

the standard deviation of each data set.
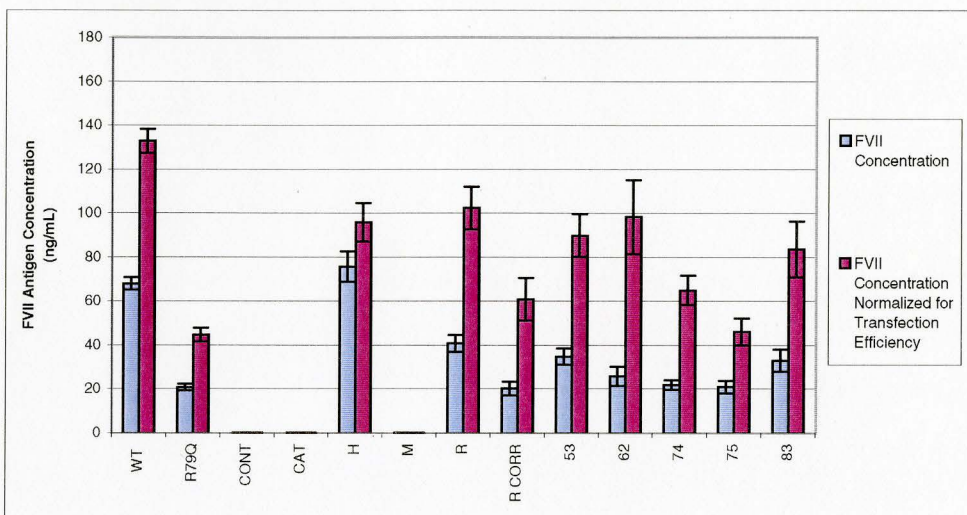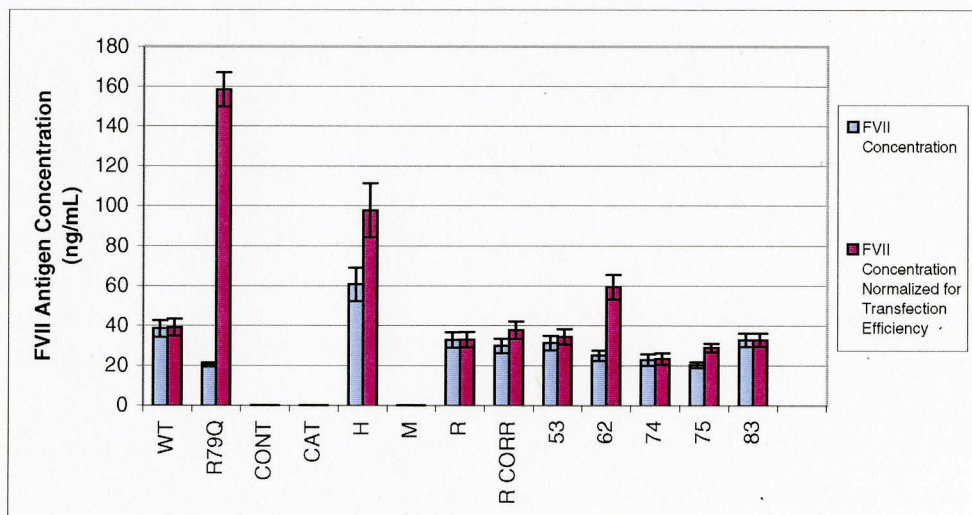
3.5 Biological Activity of the FVII Variants

3.5.1 Prothrombin Time

A standard curve was initially developed, and used as a reference to determine the clotting activity of the recombinant FVII variants (Figure 11B). The linear range of the assay was determined as clotting times between 15 and 60 seconds, and it was ensured that all clotting times used fell within these boundaries.

The clotting activities of the FVII variants are shown in Figure 11A, and are a result of the data combined from all three transfections. Wild-type human FVII had a clotting activity of 786 ± 33 U/mg FVII. The two highest clotting activities, both significantly greater than that seen with wild-type human FVII, by ANOVA, were observed for the point mutant A75D and R79Q, at 1584 ± 73 U/mg FVII and 1338 ± 68 U/mg FVII, respectively. Point mutants S53N and T83K also possessed clotting activities that were significantly greater than that of wild-type human FVII. Their activities were 1013 ± 80 U/mg FVII and 1075 ± 22 U/mg FVII, respectively. The clotting activities of the human variant "H", both the rabbit chimeras "R" and "R CORR", and the point mutants K62E and P74A were not significantly different than that of wild-type human FVII. The control transfection, the CAT-only construct and the mouse chimera showed no significant clotting activity.

Figure 11: Clotting Activity of rFVII Variants. **(A)** The clotting activity, expressed in units per milligram FVII and determined from the prothrombin time, is shown for all of the FVII variants. Data presented is an average of that obtained from the three transfections conducted. Error shown is the standard deviation of each data set. **(B)** Standard curve used to determine the clotting activity of the FVII variants.
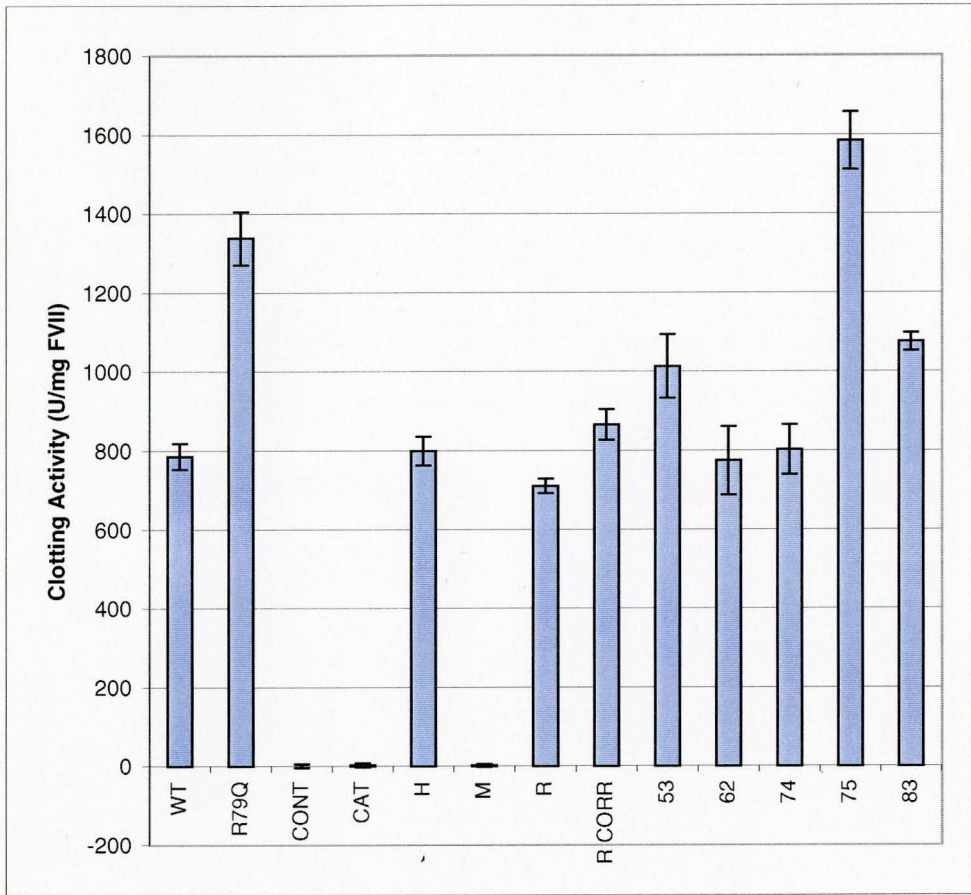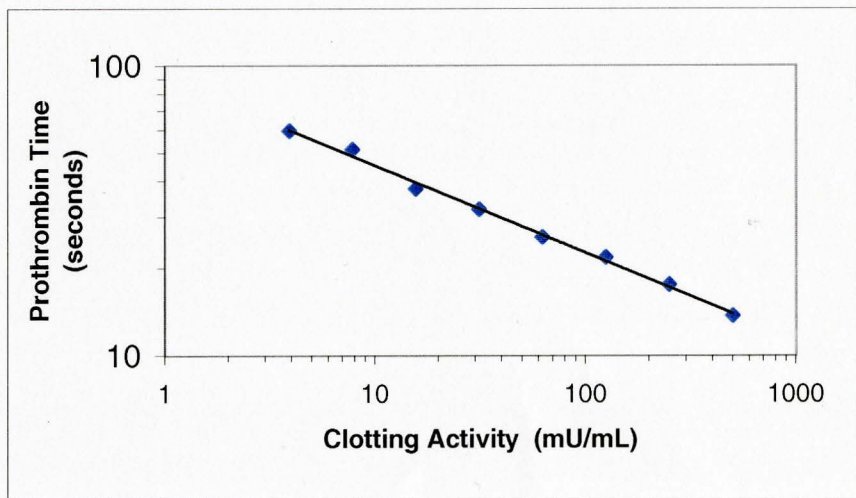
3.5.2   Amidolytic Activity

There was no standard curve generated for the amidolytic assay. Instead, 2 concentrations of plasma-derived human FVII, 10 ng/mL and 30 ng/mL, were tested to establish that a dose response was present. The $\Delta A405nm/min$ was 3x greater at a FVII concentration of 30 ng/mL than it was with 10 ng/mL FVII, confirming a dose response in this range. A FVII concentration of 20 ng/mL was used when testing the recombinant FVII variants.

The amidolytic activities of the rFVII variants are shown in Figure 12, and are an average of the data obtained from all three transfections. Wild-type human FVII had an amidolytic activity, in terms of $\Delta A405nm/min$, of 0.074 ± 0.003. The greatest amidolytic activities were seen for R79Q and the point mutant A75D, with $\Delta A405nm/min$ values of 0.12 ± 0.006 and 0.11 ± 0.002, respectively. The point mutant K62E and the corrected rabbit chimera "R CORR" also had amidolytic activities which were slightly higher than wild type, with $\Delta A405nm/min$ values of 0.092 ± 0.004 and 0.086 ± 0.004, respectively, and both were shown to be significantly significant by ANOVA. Point mutants S53N, P74A and T83K each had amidolytic activities which were not significantly changed from that of wild-type human FVII.

Two constructs showed amidolytic activities that were significantly lower than wild type. The human variant "H" had a $\Delta A405nm/min$ of 0.062 ± 0.004. The uncorrected rabbit chimera "R" showed the lowest amidolytic activity of any construct, with a $\Delta A405nm/min$ of 0.052 ± 0.002.

Figure 12: Amidolytic Activity of rFVII Variants. The amidolytic activity, in terms of change in absorbance at 405 nm per minute, is shown for all of the rFVII variants constructed. Data presented is an average of that obtained from the three transfections conducted. Error shown is the standard deviation of each data set.
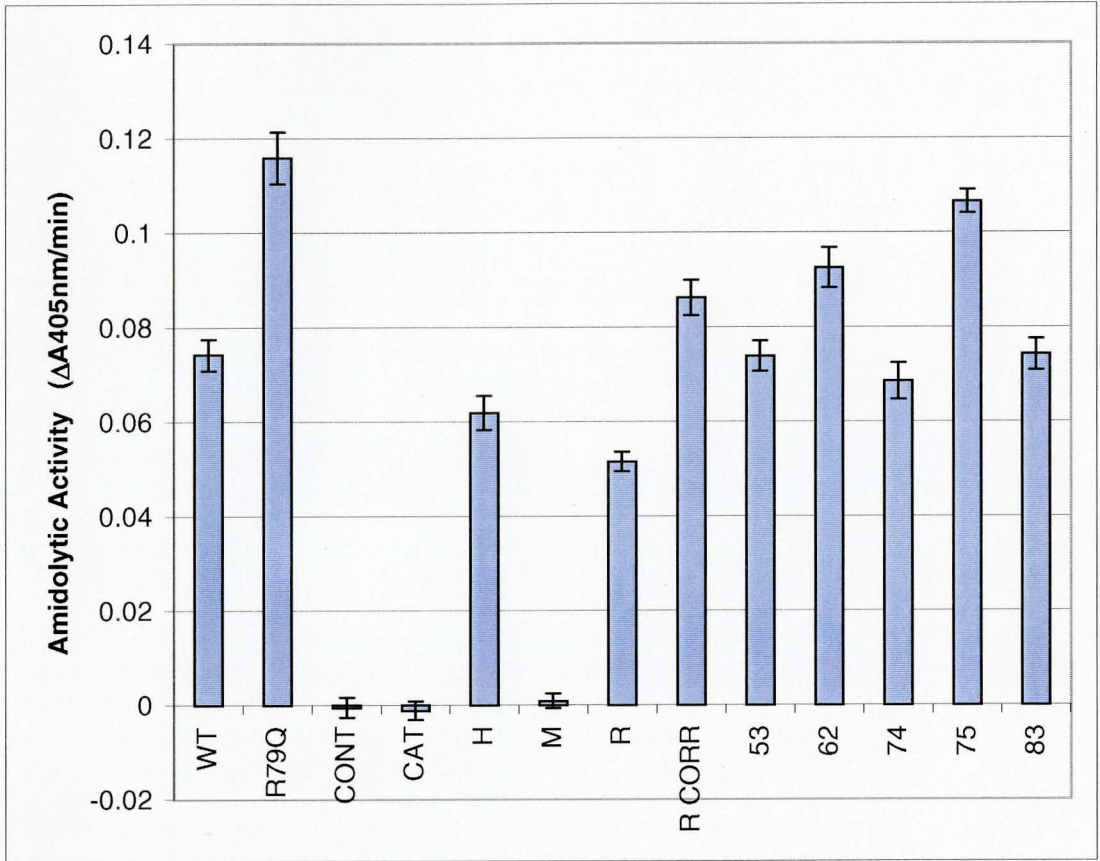
### 3.5.3 Relative Biological Activity of the FVII Variants

The relative clotting and amidolytic activities of the FVII variants are summarized in Figure 13, which was adapted from Figures 11 and 12. Values are expressed as a percentage of the activity seen with wild-type human FVII, which has been designated with 100% activity. Generally, for each FVII variant, similar activities, as a percentage of wild type human FVII, were seen with both of the biological activity assays.

Figure 13: Relative Clotting and Amidolytic Activities of rFVII Variants.

The relative clotting and amidolytic activities, as a percentage of that observed for

wild-type FVII, is shown for all of the rFVII variants constructed. Pink bars show

the clotting activity, and dark blue bars show the amidolytic activity. Data

presented is an average of that obtained from the three transfections conducted.

Error shown in the standard deviation of each data set.

Relative Activity of rFVII Variants
(as a % of wild-type FVII activity)
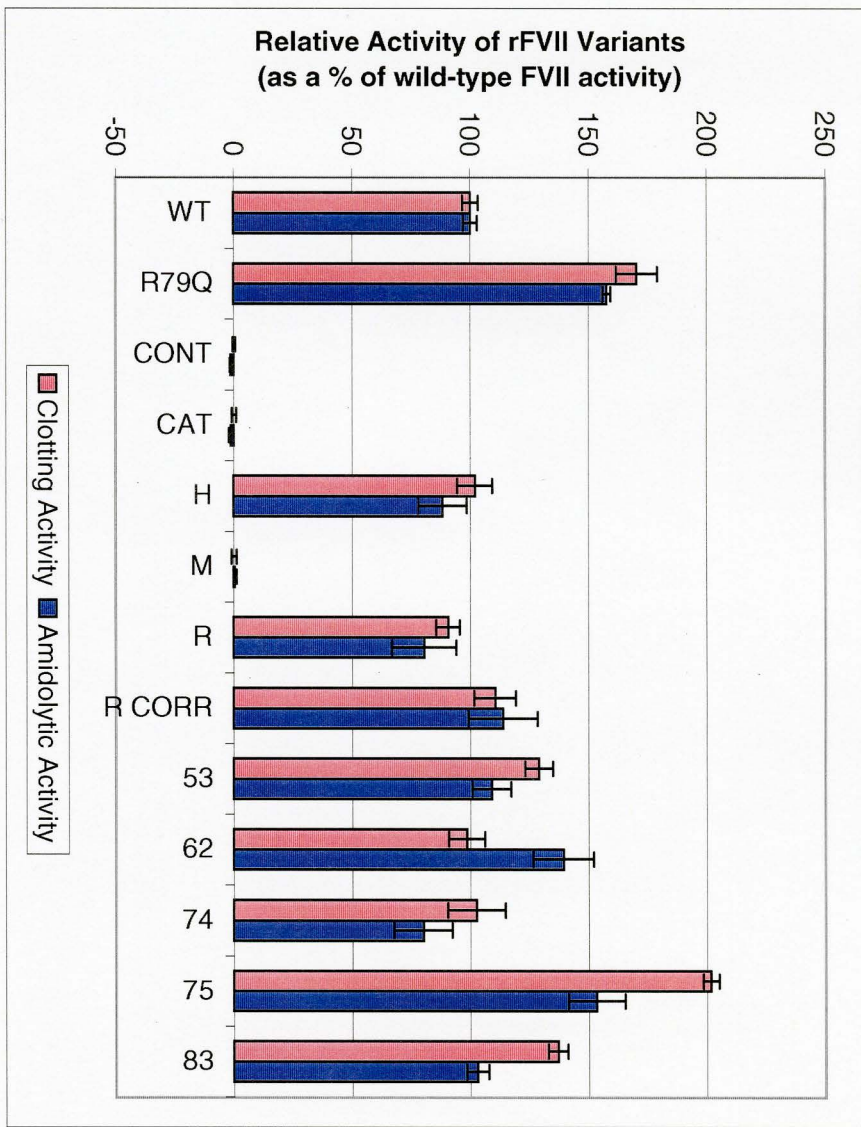
3.6   Direct TF Binding of the FVII Variants

A standard curve was initially developed to determine the linear range of the direct TF binding assay. The assay was found to be linear in the range of 2 to 25 ng/mL FVII (Figure 14B). A rFVII concentration in the tissue culture media of 20 ng/mL, which is well within the linear range of the assay, was chosen to use with the FVII variants.

Figure 14A shows the binding of the FVII variants to human TF, relative to that observed for wild-type human FVII. Data is an average of that obtained from all three transfections. Recombinant wild-type human FVII was designated as having 100% TF binding, and all other constructs were expressed as a percentage of this value. The control transfection, CAT-only construct and mouse chimera showed no significant TF binding. In addition, the uncorrected rabbit chimera "R" also showed no significant TF binding with respect to wild-type human FVII.

The greatest TF binding was seen with the A75D point mutant, at $190 \pm 19\%$ of that seen with wild type. The only other construct determined to have a significantly greater TF binding capability was point mutant T83K, at $157 \pm 10\%$ of that seen with wild-type human FVII. R79Q and the corrected rabbit chimera "R CORR" both had significantly less TF binding capability of wild-type human FVII, at $51 \pm 8\%$ and $55 \pm 11\%$, respectively. No significant differences were found in the binding of TF between wild-type human FVII and the human variant "H" or the point mutants S53N, K62E and P74A.

Figure 14: Direct TF Binding of rFVII Variants. **(A)** The ability of the rFVII variants to bind human TF, as a percentage of that seen with wild-type hFVII, is shown for all of the rFVII variants constructed. Data presented is an average of that obtained from the three transfections condu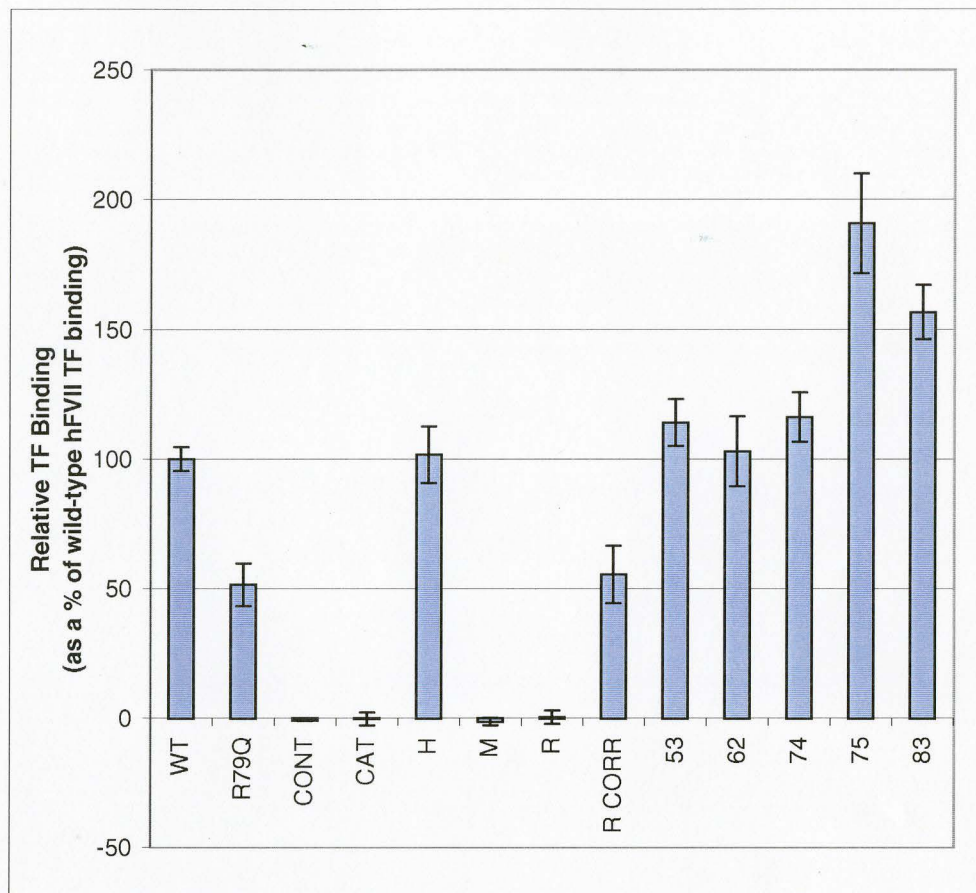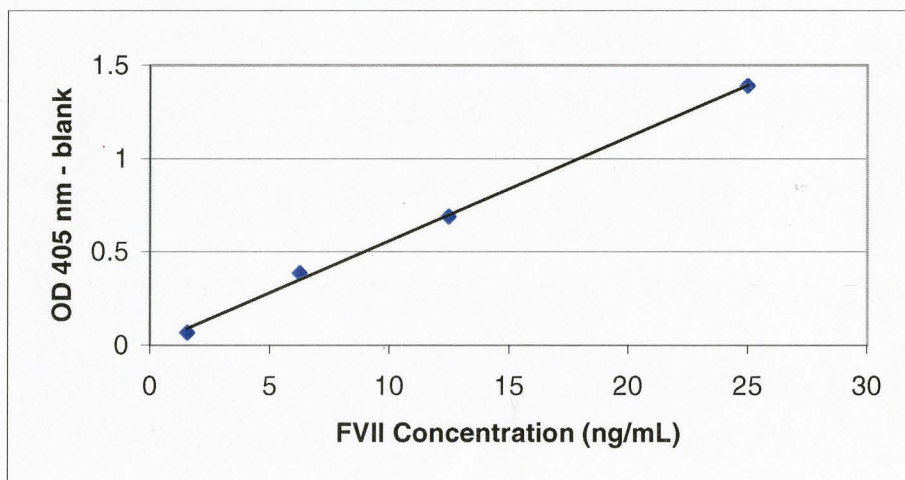cted. Data shown is the standard deviation of each data set. **(B)** Standard curve to show the linear range of the assay.

3.7   Computer Modeling of the Structures of the FVII Variants

Structures of the human FVII point mutants A75D and T83K were predicted

using Swiss-Pdb Viewer. Figure 15 is a computer-generated prediction of the A75D

mutation, showing amino acid residues that are located within 5 Å of the central carbon

of the amino acid backbone at position 75. The upper panel shows wild-type FVII while

the lower panel shows the predicted structural result of this mutation. The

alanine→aspartic acid substitution at amino acid 75 introduces an additional carbonyl

group, and therefore a polar negative charge, to the molecule. Within the dimensions

shown, it appears that there are no additional bonding interactions as a consequence of

this substitution. The additional charged oxygen atom introduced does appear to be

within close proximity of the amine nitrogen seen on the lysine residue at position 85,

although the computer prediction does not show any interaction which would change the

protein conformation. This apparent closeness in proximity may be due to the relative

orientation of the 2 atoms as a result of the picture, and may not be as true as anticipated.

Figure 16 illustrates a similar view to figure 15, but shows all interactions both

within the FVII molecule and between FVII and TF, within a 10 Å range of amino acid

75 of FVII. Here the chains are not colored by atom, but rather by protein. The TF chain

is shown in blue and the FVII chain is shown in white. Again the upper panel shows

wild-type human FVII while the lower panel shows the predicted structural effect of the

A75D mutation. From this view, this amino acid change may introduce an additional

interaction within the FVII molecule. This interaction, from left to right on the figure,

occurs between the distal oxygen atoms of the aspartic acid residues at positions 86 and

75, and is at a distance of 2.38 Å. This repulsive force between the 2 oxygen atoms could consequently introduce a conformational change within the FVII molecule that results in increased TF binding.

Figure 17 is a computer-generated prediction of the T83K mutation, showing amino acid residues that are located within 5 Å of the central carbon of the amino acid backbone at position 83. The upper panel shows wild-type FVII while the lower panel shows the predicted structural result of this mutation. The threonine→lysine substitution at amino acid 83 results in the elimination of a hydroxyl side chain and the introduction basic side chain with an additional amine group. The predicted structural effect of this change is the elimination of an interaction between oxygen atoms from the threonine at amino acid 83 and the glutamic acid at amino acid 77.

Figure 18 illustrates a similar view to figure 17, but shows all interactions both within the FVII molecule and between FVII and TF, within a 10 Å range of amino acid 83 of FVII. Here the chains are not colored by atom, but rather by protein. The TF chain is shown in blue and the FVII chain is shown in white. Again the upper panel shows wild-type human FVII while the lower panel shows the predicted structural effect of the T83K mutation. From this view, the amino acid change may introduce an additional hydrogen bond between FVII and TF. This interaction is predicted to occur between the sulphur atom of the cysteine residue at amino acid 49 in TF and the amine group of the lysine residue at amino acid 83 in FVII, at a distance of 2.72 Å. The presence of an additional hydrogen bond would clearly account for the increased TF binding observed with this FVII mutant.

Figure 15: Predicted Structure of Human FVII A75D. **(A)** A computer

prediction of the structure of human FVII, showing all amino acid residues within

5 Å of the central carbon at amino acid 75. Carbon residues are in white, nitrogen

residues are in blue and oxygen residues are in red. Hydrogen bonds are shown

with orange dotted lines, and their lengths indicated. Relevant atoms are labeled

accordingly **(B)** A computer prediction of the structure of human FVII A75D,

showing all amino acids within 5 Å of the central carbon at position 75. Atoms

are colored as in panel A.

A
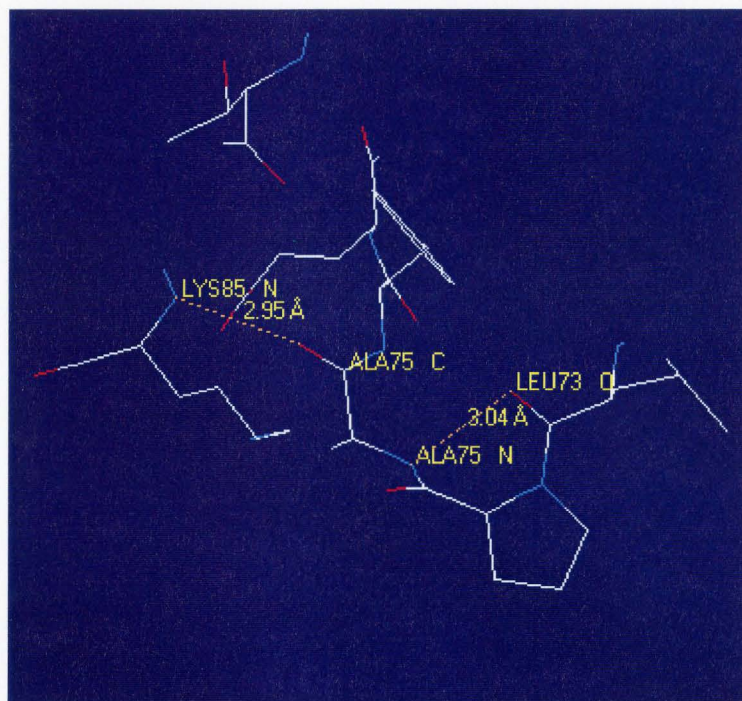
B
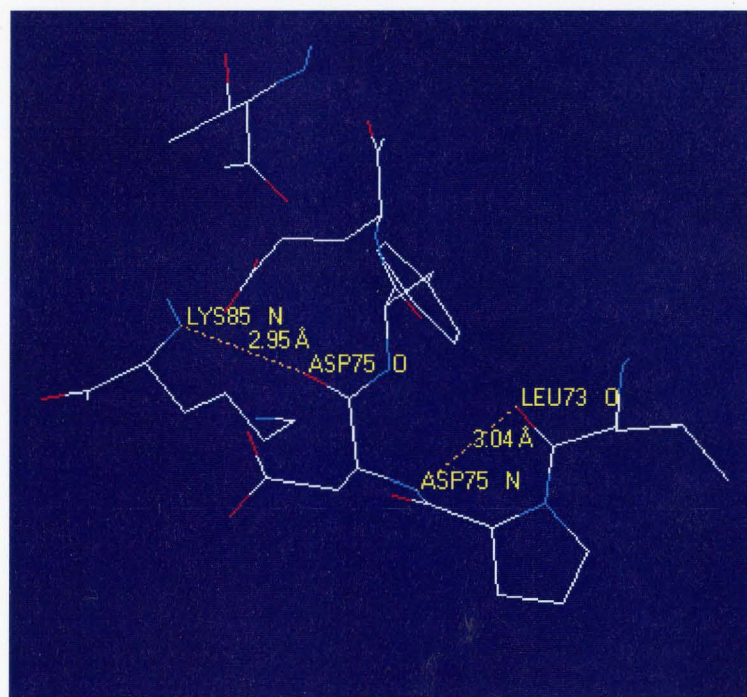
Figure 16: Predicted Structure of Human FVII A75D with TF. (A) A computer prediction of the structure of human FVII in complex with TF, showing all amino acid residues within 10 Å of the central carbon at amino acid 75. The FVII chain is colored white and the TF chain is colored blue. Hydrogen bonds within the FVII molecule are shown with green dotted lines. Disulphide bonds are shown in yellow. Relevant atoms are labeled accordingly **(B)** A computer prediction of the structure of human FVII A75D in complex with TF, showing all amino acids within 10 Å of the central carbon at position 83. Chains are colored as in panel A. An additional interaction within the FVII molecule, as a result of this mutation, is illustrated with an orange dotted line and its 2.38 Å length indicated.

A
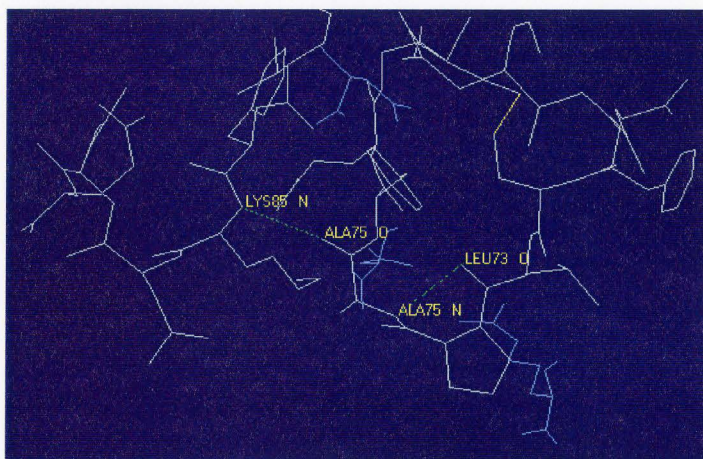
B
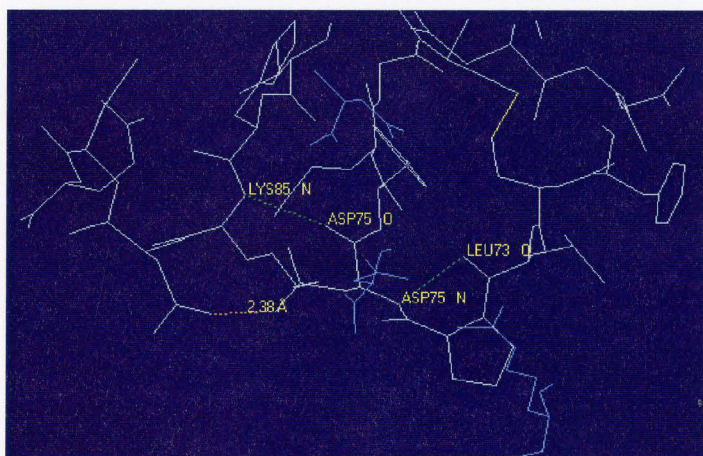
Figure 17: Predicted Structure of Human FVII T83K. **(A)** A computer

prediction of the structure of human FVII, showing all amino acid residues within

5 Å of the central carbon at amino acid 83. Carbon residues are in white, nitrogen

residues are in blue and oxygen residues are in red. The orange dotted line

represents a repulsive force observed between 2 oxygen atoms, and its 2.29 Å

distance is indicated. Hydrogen bonds are shown with green dotted lines.

Disulphide bonds are shown in yellow. Relevant atoms are labeled accordingly

(B) A computer prediction of the structure of human FVII T83K, showing all

amino acids within 5 Å of the central carbon. Atoms are colored as in panel A.

A

GLU77 N   THR83 O
         THR83 OG1
         2.29 Å
GLU77 O   THR83 N

B

GLU77 N   LYS83 O

GLU77 O   LYS83 N

Figure 18: Predicted Structure of Human FVII T83K with TF. **(A)** A computer prediction of the structure of human FVII in complex with TF, showing all amino acid residues within 10 Å of the central carbon at amino acid 83. The FVII chain is colored white and the TF chain is colored blue. Hydrogen bonds within the FVII molecule are shown with green dotted lines. Disulphide bonds are shown in yello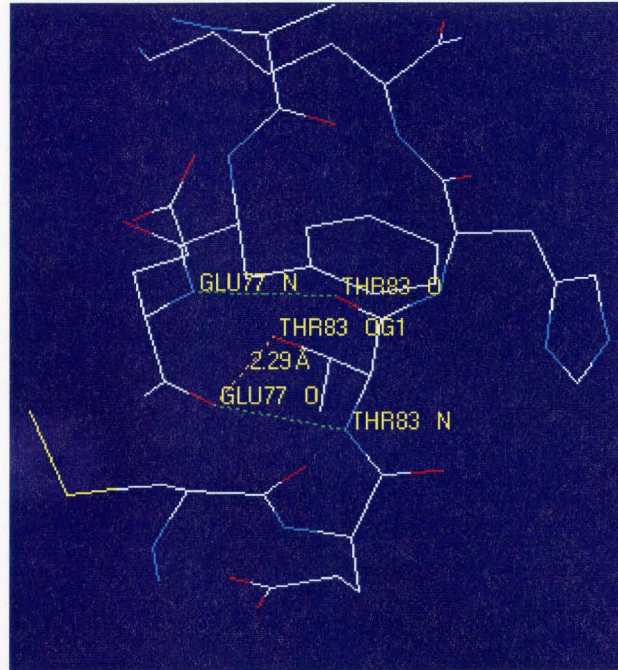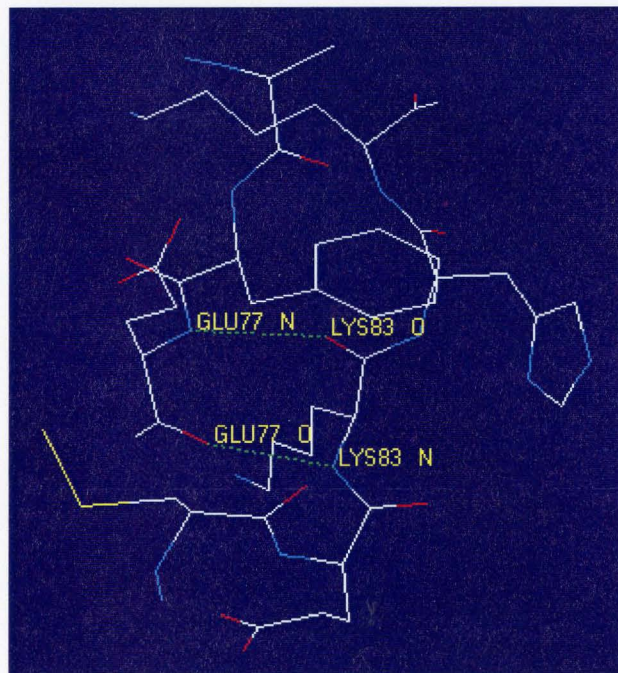w. Relevant atoms are labeled accordingly **(B)** A computer prediction of the structure of human FVII T83K in complex with TF, showing all amino acids within 10 Å of the central carbon at position 83. Chains are colored as in panel A. The additional hydrogen bond between FVII and TF, as a result of this mutation, is illustrated with an orange dotted line and its 2.72 Å length indicated.

A
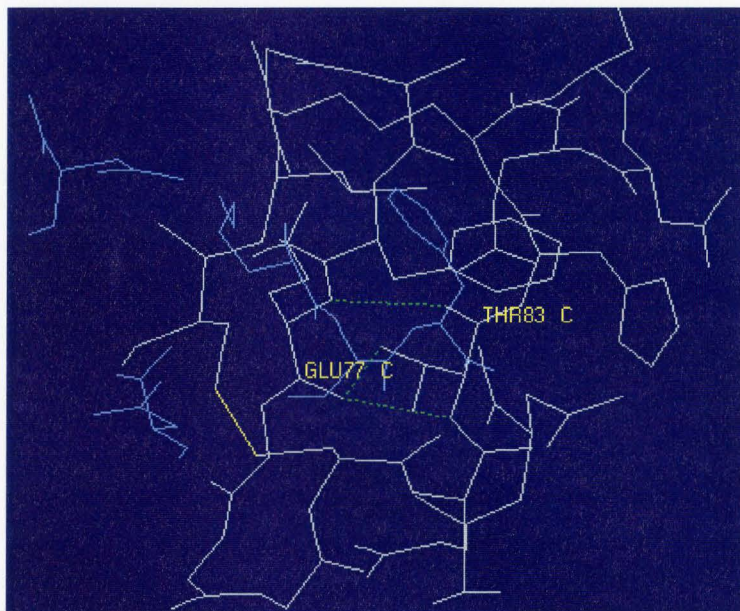
B
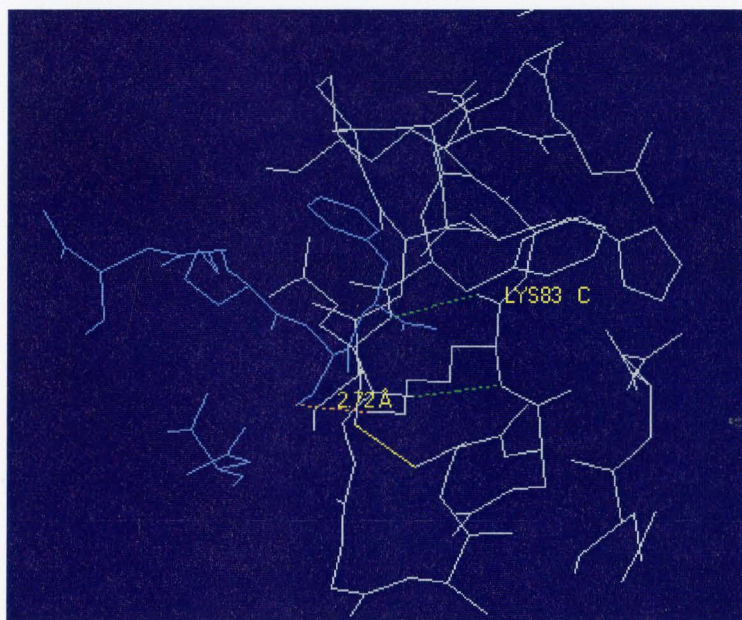
4.0 DISCUSSION

4.1   Strategy to Create a FVII Variant With an Increased TF Affinity

We initially hypothesized that by changing amino acid residues within the EGF-1 domain of human FVII to those residues natively found in other species, it might be possible to generate a FVII protein with increased TF binding. This could be done through the exchange of the entire EGF-1 domain, or through the mutation of individual amino acid residues within this module. One potential application of a FVII molecule with increased T binding, when combined with active site inhibition, would be a new competitive inhibitor of the extrinsic pathway of coagulation. This novel agent would act on the initiating event of the extrinsic pathway rather than as most antithrombotics do, later in the coagulation cascade.

Results of a study by Janson *et al* prompted this work. These investigators found that when combined with human TF, plasma from the mouse and rabbit species were able to clot 13x and 4x faster, respectively, relative to the homologous human system (24). Though many reasons may explain this phenomenon, one hypothesis is that it is due to an increased affinity of the FVII from the mouse and rabbit for human TF. As it is the complexing of FVII and TF which initiates the extrinsic pathway of coagulation, an increased affinity of the plasma from either the mouse or rabbit species for human TF could in turn increase the rate at which a fibrin clot is formed. Within the plasma system however, there is a full complement of the clotting factors present. It can not be assumed that it is in fact FVII, and in particular the EGF-1 domain of FVII, that is responsible for

phenomenon seen by Janson et al. Assuming the interaction of FVII and TF is responsible for these observations suggests that the difference in clotting activity seen was due to the EGF-1 domain of the FVII molecule. Much research has implicated the FVII EGF-1 domain as important in the tight binding of the FVIIa•TF complex (8, 9, 21, 35), with the publication of the crystal structure of soluble TF in complex with FVIIa confirming this. Greater than 43% of the FVII residues which contact TF in the FVIIa•TF complex are located within the EGF-1 domain (1). Consequently, to have a FVII molecule with an increased TF affinity as compared to wild-type human FVII is probably due to an interaction within this region.

The primary role of EGF-like domains is the mediation of protein-protein interactions (5). These modules have also been shown to act as structural units within many of the trypsin-like serine proteases. The vitamin K-dependent coagulation factors VII, IX and X, as well as protein C, each possess two EGF-like domains (11). The conservation of these modules between proteins demonstrates their importance in both protein structure and function. By altering the residues within this region, it was hypothesized that there would be an effect on the interaction seen between FVII and TF. In addition to the conservation of structure observed with many of the vitamin K-dependent proteins involved in the coagulation cascade, there is also a conservation of amino acid composition. A high degree of sequence homology is observed between the EGF-1 domains of human coagulation factors VII, IX and X (7). Many of the residues are conserved between at least two of the three proteins, if not all. Six cysteine residues are consistently located in the same amino acid positions within each of these proteins.

This homology can be further extended to the FVII EGF-1 domain from various species. When comparing the FVII EGF-1 domain from human, mouse, rabbit and bovine, 26/38 amino acid residues are identical between all species. Of the residues that differ, identical residues are often found in two or more of the species (22).

For these reasons, it was decided to generate chimeric FVII molecules in which the EGF-1 domain from human FVII was exchanged for the FVII EGF-1 domain from mouse or rabbit, either in its entirety or only with respect to individual amino acid residues. This approach ensured that the residues necessary for the structure of the protein were conserved while the altered amino acids were those that are variable between the species. Typically the unconserved residues impose the specificity of the protein, guiding its protein-protein interactions. Changing the amino acid residues of the FVII EGF-1 domain in such a manner may create a chimeric FVII that maintains its protein structure but acquires the binding interactions of the species from which its residues originated. This potentially would lead to a human FVII variant with an increased TF binding affinity.

The initial constructs made were the mouse and rabbit chimeras. These proteins consisted of the human FVII molecule with its native EGF-1 domain exchanged for that of mouse or rabbit FVII. Five human FVII point mutants were also constructed. These incorporated individual amino acids substitutions to the FVII EGF-1 domain in which the native residue was changed to that seen in rabbit FVII. All FVII variants constructed are summarized in Appendix A. Each of the FVII variants constructed was transiently expressed and tested for FVII antigen secretion into tissue culture media. This

conditioned culture media was tested for FVII biological activity by determining the

prothrombin time and amidolytic activity of the recombinant FVII variants. In tandem,

these assays are very effective in demonstrating the biological activity of FVII. Finally

the ability of the FVII variants to bind human TF was examined. Constructs that

exhibited significantly different TF binding relative to wild-type human FVII were

computer-modeled to predict the possible interactions responsible for the differences

observed.

4.2   Construction of the FVII EGF-1 Domain Exchange Chimeras

To facilitate the subcloning of the FVII EGF-1 domain from mouse or rabbit into

the human FVII molecule, it was necessary to generate restriction sites via site-directed

mutagenesis. In each case, BstEII and NsiI sites were generated at the 5' and 3' ends,

respectively, of the EGF-1 domain. The creation of the BstEII site involved a single base

pair change at amino acid 46. This was a G→T substitution at the wobble position that

generated only a silent mutation and still coded for a glycine. Creating the NsiI site

required 3 base pair changes. These were AA→TG changes in the latter two positions of

amino acid 83 and a C→T substitution at the wobble position of amino acid 84. The

C→T substitution created only a silent mutation, still coding for a histidine at amino acid

83. The AAA→ATG at amino acid 83, the final residue of the FVII EGF-1 domain,

coded for an amino acid change from a lysine to a methionine.

After the exchange of the EGF-1 domains, all of the mutations created by the site

directed mutagenesis, silent or not, were to be corrected. This was accomplished with the

rabbit chimera, where at the 5' and 3' ends of the EGF-1 domain the BstEII and NsiI

sites, respectively, had their native nucleotide sequences reintroduced. With the mouse

chimera a great deal of difficulty was encountered during the second round of

mutagenesis, during which time these base pairs were to be changed back to the native

ones. After multiple unsuccessful attempts at the simultaneous correction of the BstEII

and NsiI sites, it was attempted to change only the latter. To change both required the

use of three primers at the same time, two for mutagenesis and one for selection, as the

use of additional primers exponentially decreases the success rate of the mutagenesis

reaction (40). By changing just the NsiI site only two primers were used, one mutagenic

and one for selection. This did not help, as many colonies were obtained after the final

transformation but none of the 48 chosen were found to have the desired mutation.

Finally, the mutagenesis was attempted using only a single primer, one for the

mutagenesis of the NsiI site only. Since this site correction involved the elimination of a

restriction site, it should have been possible to use this site elimination as the selection

site also. This method still yielded an acceptable number of colonies after the final stage

of mutagenesis but none were found to have incorporated the desired mutation (of 48

colonies chosen for analysis).

An alternative bacterial strain was also employed during the final mutagenesis

transformation. Originally XL-1 Blue cells had been used and these were substituted by

DH5α. This strategy made no improvement and it was decided to continue with the

constructs that had been successfully completed, designated as "M" and "R CORR". The

mouse chimera "M", is human FVII with the mouse EGF-1 domain, but which still has

the BstEII and NsiI sites at the 5' and 3' ends, respectively, of the EGF-1. Therefore

there is a lysine→methionine substitution at amino acid position 83. The rabbit chimera, "R CORR", is human FVII with the rabbit EGF-1 substituted, in which the BstEII and NsiI sites have been successfully changed back to the native residues, and all of the desired amino acids are in place.

There were multiple reasons for changing the BstEII and NsiI sites back to their original nucleotide sequences. Restoration of the BstEII site was not essential, as this change did not involve an amino acid substitution. The same was true with the single base pair change at amino acid 84. Since the two base pair changes at position 83 also coded for an amino acid change, it was necessary to change these nucleotides back to their native nucleotides in order to achieve the desired human FVII EGF-1 domain exchange chimera. While the lysine→methionine substitution did not generate a true human FVII mouse/rabbit EGF-1 chimera with the native residues, an special consideration had to me made from a protein function aspect. As well as coding for internal methionine residues, the ATG codon forms a part of the initiation signal of translation. Methionine is a relatively uncommon amino acid, with an average occurrence in proteins of 2.2%. Since it always comprises the initiator codon, this makes the presence of methionine within the interior of proteins sequences even less common than may initially appear. By introducing an alternative site for translation initiation, translation could start downstream of the real initiation site. This would result in the synthesis of a truncated version of the protein and would ultimately inhibit proper protein function, if protein synthesis and secretion were even possible.

As the methionine residue at amino acid 83 of the mouse chimera could not be corrected it was necessary to account for this amino acid substitution by other means, and two other constructs were made to assist in the analysis of the FVII variants. The first is the rabbit chimera designated as "R". This is the human FVII molecule with the rabbit EGF-1, but which still has the BstEII and NsiI sites present. These include the silent mutations at amino acids 46 and 84, as well as the lysine→methionine substitution at amino acid 83. This variant was included to see if the methionine residue within the rabbit chimera introduced variations in protein function. Results obtained from the biological and binding assays with "R" and "R CORR" could be compared, and any significant differences could possibly be accounted for by this change. These variations could be extended to the mouse chimera, aiding in the formation of hypotheses about how it would function without the restriction site present. In the end this was not necessary however, as the transfected mouse chimera was unable to secrete FVII antigen and was used only as an additional negative control.

The human variant "H" was also used in the analysis of the EGF-1 domain exchange chimeras. This is the full-length human FVII molecule, with BstEII and NsiI sites at the 5' and 3' ends, respectively, of its EGF-1 domain. Again this generated only a silent mutation at the 5' and, while at the 3' end there is a threonine→methionine change at amino acid 83 (human FVII has a threonine residue at this position rather than the lysine seen in both mouse and rabbit FVII). This variant was created for the same reason as the uncorrected rabbit chimera "R". Results obtained for wild-type human FVII and the human variant "H", from any of the biological assays, could be compared and

significant differences observed could be attributed to the presence of the methionine residue.

4.3   Construction of the Human FVII Point Mutants

In creating the human FVII point mutants, the native amino acid residues of the human FVII EGF-1 domain were substituted by those seen in the rabbit EGF-1 domain. These changes were S53N, K62E, P74A, A75D, and T83K. The serine→asparagine substitution at amino acid 53 involved 2 neutral amino acids with uncharged polar side chains. Serine contains a hydroxyl group, and asparagine contains additional amine and carbonyl groups. Both residues have the capability to form hydrogen bonds, due to the presence of lone electron pairs. The lysine→glutamic acid substitution at amino acid 62 involved the change from a basic amino acid to an acidic amino acid. Lysine possesses an additional amine group that carries a positive charge, while glutamic acid possesses an additional carbonyl group, which carries a negative charge. This negative charge gives the amino acid its polarity, and consequently water will be able to surround the molecule. Lysine is given its polarity from the amine group, which shows the capacity to yield a proton. At amino acid 74, the proline→alanine substitution involved 2 amino acids with non-polar side chains. The structural difference is that alanine adds only a single methyl group the amino acid backbone while proline has a ring structure which joins 3 additional methyl groups to the backbone. The alanine→aspartic acid substitution at amino acid 75 involved the change from an uncharged non-polar amino acid with one methyl group added to the amino acid backbone to a charged polar amino acid with an acidic side chain resulting from the presence of an additional negatively charged carbonyl group. The

biggest difference seem between these 2 residues is the inability of alanine to interact

with water, as opposed to the natural tendency of aspartic acid to surround and interact

with water due to its negative charge. The mutation at amino acid 83 involved a

threonine→lysine substitution, in which an uncharged polar amino acid was changed to a

basically charged polar amino acid. Threonine has 2 methyl groups as well as a hydroxyl

group, which is responsible for its ability to interact with water. Lysine contains multiple

methyl groups as well as an additional amine group that carries the positive charge, and

gives lysine the ability to yield a proton.

The other difference seen between the rabbit FVII EGF-1 and the human FVII

EGF-1 domain is at amino acid 65. Rabbit FVII natively has an isoleucine while human

FVII has a leucine. This mutation was not created, as the only difference between these 2

molecules is in the relative orientation of the methyl groups. It was not suspected that

such a change would cause a large difference in protein synthesis. Without changing the

side chains of the amino acid, no additional secondary and tertiary structures were

expected within the protein, and consequently it was hypothesized that there would be no

effect on protein synthesis and/or secretion.

4.4   Transient Expression of the FVII Variants

Preliminary experiments involved the transient expression of the mouse and rabbit

chimeras into HEK 293 cells. The wild-type human FVII and FVII R79Q controls were

secreted at expected levels (28, 48) but FVII antigen levels were very low with the rabbit

chimera, and undetectable with the mouse chimera. A second attempt was made at this

transfection which yielded the same results. These chimeras were subsequently

transfected into BHK cells. It was hypothesized that an alternative cell line may assist in

protein synthesis and/or secretion. Although HEK 293 cells are commonly used for

transient expression experiments involving FVII and other vitamin K-dependent proteins

(7, 10, 25, 28), other cell lines, including BHK, have successfully been employed (46).

As no significant differences in protein secretion were seen between the 2 cells lines, a

return was made to the HEK 293 cells.

It was hypothesized that the exceptionally low levels of FVII secretion by the

chimeras may be due to an incompatibility of the exchanged EGF-1 domain and human

FVII. The exchanged domain may have imposed a conformational change of the FVII

molecule that hindered protein synthesis or secretion, and therefore no FVII would be

expected in the conditioned culture media. This did not seem a probable explanation

however, as so many chimeric vitamin K-dependent proteins have been constructed in

which the native EGF-1 domain of one vitamin K-dependent protein has been exchanged

for that of another. These chimeras have involved a variety of domain exchanges between

factors VII, IX and X as well as protein C. Each of these chimeras was capable of protein

synthesis after transient expression despite their variable biological activities (7, 29, 53).

Additionally, by exchanging the FVII EGF-1 domain with that from various species, the

conserved residues necessary for protein structure were not altered. This would predict

that the chimeric protein should retain a structure that permits proper protein synthesis

and secretion. Despite these expectations, the lack of proper protein secretion with the

chimeras appeared to be due to one or more of the amino acid changes seen between the

EGF-1 domain of mouse or rabbit FVII and those of human FVII. The change could

have imposed a very specific, localized effect within the FVII molecule. This was the rationale behind creating the human FVII point mutants.

The human FVII point mutants were originally generated to investigate the finding that the mouse chimera was unable to secrete FVII protein and that the rabbit chimera was only able to secrete FVII at very low levels after transient expression. The focus was on the amino acid changes between the rabbit and human FVII EGF-1 domain for 2 reasons. First, fewer differences exist between the rabbit and human FVII EGF-1 domains than between the mouse and human FVII EGF-1 domains, and therefore fewer mutants had to be made. Within the FVII EGF-1 domain 6/38 amino acids vary between the rabbit and human species, and 10/38 differ between the mouse and human. Second, even though FVII secretion levels were low, some FVII antigen was detected after transfection with the rabbit chimera. With the mouse chimera no FVII was detected after transient expression, suggesting a more complicated protein structure problem that may not have been resolvable by constructing individual point mutations. The amino acid substitutions were made from the native human FVII residues to the rabbit FVII residues, rather than vice versa, to investigate individual effects of each amino acid change. If the low FVII synthesis in the rabbit chimera was a consequence of multiple residues, they would be unidentifiable by individually mutating each from the rabbit residue to the human residue. Acting in the reverse order would show if any individual amino acids had a gross effect on protein secretion. Later, if desired, multiple mutations could be incorporated simultaneously.

After constructing the point mutants, it was found that large deletions of the FVII sequence existed in each of the chimeras. The mouse chimera was missing approximately 2/3 of its EGF-1 domain, and had additional small deletions, 4-8 amino acids in length, throughout the length of the FVII gene. The rabbit chimera also had deletions, though far less than the mouse chimera. These deletions were typically 3 to 6 amino acids in length and occurred throughout the FVII sequence, including some within the EGF-1 domain. These deletions clearly accounted for the low FVII levels seen in the total FVII antigen ELISA. With large portions of the FVII gene missing, protein synthesis would ultimately be affected, resulting in either no or low levels of FVII present in the transfected media. Additionally, a polyclonal rabbit α-human FVII antibody was used for the total FVII antigen ELISA. If its epitopes targeted one or more of the areas which were missing from the sequence, then FVII would not be detected, even if there was some present. The rabbit and mouse chimeras were reconstructed with the incorporation of a few changes to assist in correcting the apparent plasmid instability problems. These included using the cloning vector pUC19 instead of pGEM3 for all mutagenesis reactions, as well as transforming the chimeras, with the exception of the initial mutagenesis transformation into BMH 71-18*mutS,* into XL-1 Blue. Previous experiences from our lab found that these were the most compatible hosts for FVII. Incorporating these changes, the chimeras were successfully reconstructed and used in subsequent transfection experiments.

The realization it was the integrity of the transfected DNA that was responsible for the FVII levels observed in the total antigen ELISA for the chimeras changed the

rationale behind using the human FVII point mutants. These mutants were no longer

needed to investigate the cause of the FVII levels observed with the chimeras, but as they

were already constructed, each point mutant was transfected and assessed for protein

synthesis and biological activity along with the FVII EGF-1 domain exchange chimeras.

After optimization of the transfection conditions, FVII antigen secreted after

transient expression of each of the FVII variants was typically between 20 and 40 ng/mL.

These FVII levels are consistent with those historically seen in our lab (28, 48). One or

two constructs in each transfection were often secreted at higher levels, between 60 and

75 ng/mL. The construct that generated these elevated levels of FVII secretion was not

consistent between the experiments, and consequently it was determined that this

variability was due to transfection efficiency rather than a phenomenon of the specific

FVII variant. After reconstruction of the FVII EGF-1 domain exchange chimeras the

rabbit chimeras "R" and "R CORR" were secreted at levels comparable to those seen

with the other FVII variants, while the mouse chimera still failed to secrete FVII. The

apparent protein synthesis and/or secretion problems exhibited by the mouse chimera

raised concern. The plasmid DNA was quantified again by spectrophotometric

absorbance at 260 nm, and the concentration was confirmed to be the same as that

initially determined. This showed that the low FVII level was not due to the fact that the

transfection was conducted with an inappropriate quantity of DNA. The plasmid DNA

was also examined on an agarose gel where it was confirmed to be the correct size and

without any impurities. The possibility exists that this chimera has once again lost part of

its FVII gene. This problem was apparently corrected, as the rabbit chimeras were being

secreted at acceptable levels, however no subsequent sequencing of this chimera has been done since the initial sequencing reactions.

Transfection efficiency of the mouse chimera was considered. In the first transfection it was the mouse chimera which was transfected with the greatest efficiency of all of the FVII variants. In each of the latter 2 transfections the mouse chimera was transfected with approximately 50% efficiency, a rate similar to that seen with many of the FVII variants which exhibited no problems with FVII secretion. This provided conclusive evidence that transfection efficiency was not the reason for the lack of protein secretion by the transfected mouse chimera. Consequently, the mouse chimera was used as an additional control in subsequent assays, in tandem with mock-transfected media and CAT-only transfected media.

4.5   Characterization of the FVII EGF-1 Domain Exchange Chimeras

No significant difference was seen, as determined by ANOVA analysis, in the clotting or amidolytic activity of wild-type human FVII compared with the human variant "H". This suggested that the methionine residue located at the 3' end of the EGF-1 domain did not interfere with protein translation. With the human variant "H", the substitution at amino acid 83 is a threonine to methionine residue. By computer modeling of this mutation, there are no significant bonds broken or formed, either within the FVII molecule or between FVII and TF, as a consequence of this change (figure not shown). This lack of structural change is consistent with the minimal difference seen between the activity of these 2 constructs. A change in bonding interactions would ultimately effect TF binding through the formation of additional hydrogen bonds between

the molecules or the generation of interactions within FVII itself that cause

conformational changes. Depending on their nature, these bonds would either enhance or

inhibit the interactions between FVII and TF, ultimately affecting the formation of the

FVIIa•TF complex. Without a change in bonding interactions it would not be expected

that there would be a significant change in TF binding. This is confirmed by the results

of the direct TF binding assay, where no significant difference is seen between the

affinity of wild-type human FVII and the human variant "H" for TF.

A statistically significant difference was found in the clotting activity of the

corrected rabbit chimera "R CORR" compared to the uncorrected rabbit chimera "R",

which still had the methionine at the 3' end of its EGF-1. "R CORR" clotted with an

approximately 20% greater efficiency, which suggested that the methionine residue did

play a role in protein function, with respect to clotting activity. Since significant clotting

activity still existed, in addition to significant FVII secretion as determined by ELISA,

this amino acid substitution did not appear to interfere in translation initiation, but rather

in protein structure and function. These results were confirmed with the amidolytic

assay. The uncorrected rabbit chimera "R" had a slightly lower, while statistically

significant, amidolytic activity than that seen with the corrected rabbit chimera "R

CORR".

The methionine→lysine substitution seen between the uncorrected rabbit chimera

and the corrected rabbit chimera, respectively, involves the change from a sulphur-

containing non-polar amino acid to a basic amino acid that carries a negative charge. As

a consequence of these structural differences, each residue has the potential for different

interactions with surrounding amino acid residues. If there are sites in the TF molecule oriented relatively near to position 83 of the FVII molecule which are capable of interactions with the free amine group of the lysine residue, then an increased interaction between these 2 molecules would be possible. The potential for an additional interaction between FVII and TF with the corrected rabbit chimera "R CORR" as compared to the uncorrected rabbit chimera "R" can be seen in the predicted structure of the human FVII point mutant T83K (see Figure 18). "R CORR" consists of the human FVII molecule with the EGF-1 domain exchanged for that of the rabbit. At the 3' end of the EGF-1 domain, only 1/8 amino acids differ between the human and rabbit species, and that is at position 83. From this perspective, it can be seen that within 10 Å units of FVII amino acid 83, as shown in Figure 18, "R CORR" is the exact same construct as the human FVII point mutant T83K, and all of its structural features may be synonymous between these 2 constructs. As a consequence of the methionine→lysine substitution, a 2.72 Å bond is predicted to have formed between the lysine residue of FVII at amino acid 83 and the cysteine residue at amino acid 49 of TF. If this prediction is correct, there would be an increased TF binding for the latter mutant, which would lead to increased clotting and amidolytic activity. Differences in TF binding between the "R CORR" chimera and the T83K human point mutant are accounted for by the variability seen between the amino acid residues of these 2 constructs at the 5' end of the EGF-1 domain.

While these predictions account for the different TF binding capabilities of the rabbit chimeras, they could not fully explain the results of the direct TF binding assay. With equimolar amounts of the FVII variants used, the corrected rabbit chimera was still

capable of binding TF, although only at one-half of the rate seen with wild-type human FVII. In contrast, the uncorrected rabbit chimera "R" showed no TF binding ability. The lysine→methionine clearly caused some additional interaction between the "R CORR" chimera and TF that resulted in an increased affinity of each protein for the other. However, without TF binding, the uncorrected rabbit chimera "R" should not exhibit any clotting or amidolytic activity, as FVII is virtually inactive when not complexed to its cofactor, TF. Both of these activities are initiated by the tight interaction of FVII and TF to form the FVIIa•TF complex, which is essential in initiating coagulation. The 3 control transfections used, mock-transfected media, CAT-only transfected media, and the mouse chimera transfected media, each exhibited no biological activity which suggests no exogenous factors existed within the conditioned culture media that were responsible for the activity seen. Further examination is needed of the relative TF binding of the rabbit chimera "R" to draw conclusions with respect to this phenomenon.

It should be noted that different sources of TF were used in the clotting and amidolytic activity assays than was used in the direct TF binding assay. Full length commercial recombinant TF, supplied by Hemoliance and relipidated as per the manufacturer's directions, was used in both the PT and amidolytic assays, where as TF apoprotein supplied by Genentech was used in the direct TF binding assay. The primary difference between these 2 sources of TF is the presence of the phospholipids in the commercial TF and not in the apoprotein. Phospholipid membrane is essential for the activity of the FVIIa•TF complex, but not for binding of the proteins. While it is possible for FVII and TF to bind in the absence of lipid, it is not possible for them to

initiate coagulation (42). This should not have effected these experiments, as the lipid was present in all cases where it was biologically necessary. TF apoprotein was also relipidated and used during one attempt of the TF binding assay, and the results were not significantly different than those seen when the apoprotein was used alone, showing that phospholipid was not essential for this experiment. The relipidated commercial TF was used in attempts with the TF binding assay, but no dose response seen with varying FVII concentrations, in addition to a very high background, so it was not possible to continue its use in this assay. The only solution was to use the commercial TF source for the biological assays and the TF apoprotein for the TF binding assay.

4.6   Characterization of the Human FVII Point Mutants

With the human FVII point mutants, a single amino acid substitution was responsible for the difference in activity seen with each of the variants. As each possesses only a single point mutation with respect to wild-type human FVII, strong conclusions can be drawn about the relative effect of each substitution. The FVII EGF-1 point mutants S53N, K62E and P74A, each had TF binding which was not, or only slightly, significantly different than that seen with wild-type human FVII. Each of these substitutions involved only minimal change in protein primary structure. It was expected that for each of these point mutants, there would not be a significant change from that seen with wild-type human FVII in the biological activity assays either. This was not the case. With S53N the clotting activity was approximately 25% greater than that seen with wild type, though amidolytic activity was the same. The K62E mutant had the same clotting activity as wild-type human FVII, but the amidolytic activity was approximately

30% higher than that seen with wild-type. P74A also had a clotting activity that was not significantly different than wild-type human FVII, though its amidolytic activity was approximately 20% less. With each of these point mutants the reason for conducting 2 biological activity assays is emphasized, as each assay examines a specific area of biological activity and together they show the overall activity of the protein. In the event that one of the assays shows slightly greater or less activity for any individual mutant, this data can not be considered biologically significant without confirmation from the second assay. Considering this, the point mutants S53N, K62E and P74A show no significantly different activity than wild-type human FVII.

The FVII variants which showed the greatest potential to satisfy the hypothesis that by changing the amino acid residues within the EGF-1 domain of human FVII to those natively found in other species, it might be possible to create a protein with increased TF binding, were A75D and T83K. A75D has almost twice the binding affinity for human TF than wild-type FVII, while T83K binds TF approximately 50% better. Both mutants exhibited proportionally increased clotting and amidolytic activity. This was expected as it is the complexing and high affinity binding of FVII and TF that initiates the extrinsic pathway of coagulation, so the generation of a stronger interaction between these 2 proteins should result in an increased biological activity. Computer predictions of the structures of the FVII variants A75D and T83K were made in order to further analyze the reasons for the increased TF affinity seen with these constructs.

The T83K mutation to human FVII changes an uncharged polar side chain containing a hydroxyl group to a charged polar side chain containing multiple methyl

groups, as well as an additional positively charged amine group. Within 5 Å of the central carbon at amino acid 83, the major difference predicted to be conferred by this substitution is the loss of an interaction between the hydroxyl oxygen atom of the threonine and the oxygen of the glutamic acid at position 83 (see Figure 17). This interaction occurs at a distance of 2.29 Å. Since this interaction occurs between 2 oxygen atoms, it is not an attractive hydrogen bonding interaction, but rather a repulsion. This repulsion could effectively change the conformation of the molecule, with the two oxygen atoms attempting to orient themselves as far away from each other as possible. The substitution to a lysine reside potentially allows the FVII molecule to adopt a more relaxed conformation in this area. The two hydrogen bonds observed between the nitrogen atom of the glutamic acid at position 77 and the threonine oxygen at position 83, do not appear as they would have a great structural effect on the FVII molecule. In addition to the fact that these bonds are unchanged with the threonine→lysine substitution, they occur at distances of 2.99 Å and 2.89 Å, respectively, which is at the extreme end of the distance where hydrogen bonding is effective (typically less than 3 Å).

The T83K mutation also has the potential to form hydrogen bonds between FVII and TF (see Figure 18). Within 10 Å of the central carbon of amino acid 83, it is predicted that an additional hydrogen bond between FVII and TF, at a distance of 2.72 Å, is formed between the lysine at amino acid 83 of FVII and the cysteine at amino acid 49 of TF. The interaction is a result of the sulphur from the cysteine residue at position 49 of the TF molecule and the additional nitrogen from the amine group of lysine. At 2.72

Å, this distance is small enough to show a great effect between these two molecules, and strongly suggests a tighter binding of the FVII•TF complex in this area. In addition to the increased TF binding, an increased biological activity would be expected as a consequence of this mutation. When comparing the T83K point mutant to wild-type human FVII, no significant difference in amidolytic activity exists, although this mutant has a clotting activity approximately 40% greater than that seen with human FVII. When the results of these assays are considered in tandem, the T83K mutant does show a greater biological activity than that of wild-type human FVII.

The reason for the increased TF binding capability expressed by the A75D variant over wild-type human FVII is less clear. By a computer-generated prediction of the FVII structure with this substitution introduced, within 5 Å of the central carbon of amino acid 75, there appears to be no additional bonding interactions as a consequence of this substitution (see Figure 15). The change involves the substitution of a non-polar methyl side chain to a charged polar carbonyl side chain. The additional charged oxygen atom appears to be in close proximity of the amine nitrogen seen on the lysine residue at position 85, although computer modeling does not show any interaction which would change the conformation of the FVII molecule. This apparent closeness in proximity may be do to the relative orientation of the two atoms which is a result of the picture, and may not be as true as anticipated. When looking at all of the interactions between FVII and TF within 10 Å of amino acid 75 of FVII, there is an additional interaction introduced (Figure 16). At a distance of 2.38 Å, an interaction is predicted to occur between the distal oxygen atoms of the aspartic acids located at amino acids 86 and 75,

both within the FVII molecule. As this interaction is between two like atoms, it is a repulsive force between the residues. This would introduce a conformational change within the FVII molecule that may in turn affect TF binding. No direct interactions are predicted to result between TF and the residue at amino acid 75 of FVII, but this conformational change could potentially create a bonding interaction between the molecules at a more remote site (beyond the 10 Å area seen within this picture). If this was the case, then an increased TF binding by this mutant would result. Consistent with the increased TF binding exhibited by the A75D mutant in the TF binding assay, it exhibited a proportionally increased clotting and amidolytic activity. A75D showed an activity of 200% and 150% of that seen with wild-type human FVII, in clotting and amidolytic activity, respectively.

Of the human FVII point mutants constructed, none have been reported as either naturally occurring (25) or as engineered. A variety of engineered FIX molecules have also been created that incorporate various point mutations within the EGF-1 domain, but again none have included the residues at amino acids 53, 62, 74, 75, or 83. Consequently, the current results have no direct basis for comparison. It is known though that in wild-type human FVII, none of these residues are in direct contact with TF in the FVIIa•TF complex. In 1999, Jin *et al.* generated human FVII chimeras in which the EGF-1 domain was exchanged for that of FIX, and the affinity for TF of each determined (25). Four additional mutants to this chimera were subsequently made in which the residues of the FIX EGF-1 domain were changed back to those natively found in FVII. As there is a great degree of homology seen within the EGF-1 domain of these proteins,

and it was hoped that one of these chimeras would mimic the mutation seen with either the human FVII point mutant A75D or T83K. At amino acid 75, according to FVII numbering, FIX has a glycine while FVII has an alanine. At amino acid 83, FIX has a leucine while FVII has a threonine. Consequently, the TF binding affinity seen with any of the chimeras created by Jin *et al.* could not be compared directly to either of these human FVII point mutants.

The largest concern raised by this work has come with the R79Q control experiments. R79Q is a naturally-occurring human FVII mutant (52) which, according to published data, has normal FVII synthesis and secretion, but decreased TF binding and activity (9, 48). The current experiments showed a decreased TF binding by R79Q, approximately 50% of that seen with wild-type human FVII, though biological activity was dramatically increased. For both the clotting and amidolytic activity assays, R79Q had 50% greater activity than that seen with wild-type human FVII. These experiments were repeated and the same results obtained each time, and these observations can not be explained. It does not seem logical that a mutant with decreased TF binding should have increased biological activity, as the formation of the FVIIa•TF complex is essential to the biological activity of FVII. Since the purpose of R79Q in this project was to act as a control for the TF binding assay, the data for this specific assay seems acceptable. If further work were done in the analysis of the biological activity of these variants however, it would be necessary to determine why the FVII R79Q variant is generating anomalous data.

Additionally, an increased relative TF binding by either of these mutants does not guarantee their ability to compete against wild-type human FVII for TF binding. A competitive ELISA was developed in our lab that is more informative than the direct binding assay (48). The competitive ELISA shows, when combined, which protein between wild-type human FVII and a FVII variant, is able to better compete for and complex with human TF. It was originally proposed to use this assay but despite much troubleshooting, this assay was not working. As the hypothesis of this study is that through the introduction of alternative residues within the EGF-1 domain of FVII, it may be possible to generate a human FVII molecule with increased TF binding that could potentially act as a competitive inhibitor of coagulation, it is essential to determine the ability of the FVII variants to compete for TF. To draw any definite conclusions in this respect, it will be necessary to get some form of competitive binding assay working.

4.7   Conclusions

The human FVII point mutants A75D and T83K were the only FVII variants constructed which were able to satisfy the hypothesis that by changing amino acid residues within the EGF-1 domain of wild-type human FVII to the native residues found in other species, it might be possible to create a FVII protein with increased TF binding. Both mutants exhibited an increased TF binding relative to wild-type human FVII. These mutants consisted of the human FVII molecule with a single point mutation to the native rabbit amino acid at the indicated position within the EGF-1 domain. A75D was able to bind TF twice as well as wild-type human FVII and T83K bound TF at 1.5 x the affinity of wild-type. With the T833K mutation, there an additional hydrogen bond is predicted

to form between FVII and TF as a consequence of the threonine→lysine substitution.
This bond occurs between the lysine at amino acid 83 of FVII and the cysteine residue at
amino acid 49 of TF, at a distance of 2.38 Å. If this computer prediction is correct, it
clearly accounts for the increased TF affinity for human TF observed with this mutant.
The source of the increased TF affinity of the A75D is less clear. There is a predicted
conformational change introduced to FVII molecule as a consequence of the
alanine→aspartic acid substitution at amino acid 75. The introduction of an aspartic acid
residue at amino acid 75 appears to generate a repulsive force between the oxygen atoms
of the aspartic acid residues at amino acids 86 and 75, at a distance of 2.38 Å. This force
may introduce an overall conformational change to the FVII molecule which leads to the
exposure of residues at another sites, rendering then them more available to interact with
TF, thereby causing an increased binding between the 2 proteins.

The increased direct TF binding seen with these mutants does not ensure their
abilities to compete against wild-type human FVII for TF binding. To determine this, it
is necessary to have a competitive assay in which both FVII constructs are tested
simultaneously in the same system. As expected with an increased TF affinity, both
A75D and T83K exhibited a biological activity that was proportionally increased.
Consequently, in order to use either FVII variant as a competitive inhibitor of
coagulation, will be necessary to inhibit their biological activity. This can be
accomplished by active site inhibition through the use of chloromethyl ketones or by site-
directed mutagenesis of active site residues of the FVII molecule. Once this is
accomplished, the recombinant FVII variants A75D and T83K could be expressed in

mammalian cell cultures and tested *in vivo* to examine their ability to act as competitive inhibitors of coagulation in a living system. If either mutant is successful at competing against wild-type human FVII for TF binding *in vivo*, while demonstrating decreased biological activity, it could potentially be used as the foundation for the development of a new class of antithrombotics, capable of acting on the initiation stage of coagulation, rather than later in the cascade.

APPENDIX A:

Summary of the FVII Variant Constructs

Mutant	Name	Description
WT	Wild-type human FVII	Wild-type human FVII
R79Q	HFVIIR79Q	Naturally occurring mutant of hFVII R79Q, Decreased tissue factor binding
H	HFVIIT83M ("human variant")	HFVII with methionine at amino acid position 83
M	HFVII mouse EGF-1 K83M ("mouse chimera")	HFVII chimera with mouse EGF-1, methionine at amino acid position 83
R	HFVII rabbit EGF-1 K83M ("uncorrected rabbit chimera")	HFVII chimera with rabbit EGF-1, methionine at amino acid position 83
R CORR	HFVII rabbit EGF-1 ("corrected rabbit chimera")	HFVII chimera with rabbit EGF-1, all native amino acid residues
S53N	HFVII S53N	HFVII with native rabbit amino acid at position 53
K62E	HFVII K62E	HFVII with native rabbit amino acid at position 62
P74A	HFVII P74A	HFVII with native rabbit amino acid at position 74
A75D	HFVII A75D	HFVII with native rabbit amino acid at position 75
T83K	HFVII T83K	HFVII with native rabbit amino acid at position 83
CONT		Transfection negative control, mock transfection with Lipofectin only
CAT		Transfection negative control, transfected only with pCMV-CAT vector

REFERENCES

1. Banner DW, D'Arcy A, Chene C, Winkler FK, Guha A, Konigsberg WH, Nemerson Y, Kirchhofer D: The Crystal Structure of the Complex of Blood Coagulation Factor VIIa with Soluble Tissue Factor. Nature 380: 41, 1996.

2. Banner DW: The Factor VIIa/Tissue Factor Complex. Thromb Haem 78:512, 1997.

3. Birnboim HC, Doly J: A Rapid Alkaline Lysis Procedure for Screening Recombinant Plasmid DNA. Nucl Acids Res 7: 1513, 1979.

4. Bjoern S, Foster DC, Thim L, Wiberg FC, Christensen M, Komiyama Y, Pederson AH, Kisiel W: Human Plasma and Recombinant Factor VII. Characterization of *O*-Glycosylations at serine residues 52 and 60 and Effects of Site-Directed Mutagenesis of Serine 52 to Alanine. J Biol Che 266: 11051, 1991.

5. Campbell ID, Bork P: Epidermal Growth Factor-Like Modules. Curr Op Struct Biol 3: 385, 1993.

6. Chang J-Y, Stafford DW, Straight DL: The Roles of Factor VII's Structural Domains in Tissue Factor Binding. Biochemistry 34: 12227, 1995.

7. Chang J-Y, Monroe DM, Stafford DW, Birkhous KM, Roberts HR: Replacing the First Epidermal Growth Factor-Like Domain of FIX with that of Factor VII Enhances Activity in Vitro and in Canine Hemophilia B. J Clin Invest 100: 866, 1997.

8. Chiang S, Clarke B, Sridhara S, Chu K, Friedman P, Van Dusen W, Roberts HR, Blajchman M, Monroe DM, High KA: Severe Factor VII Deficiency Caused by Mutations Abolishing the Cleavage Site for Activation and Altering Binding to Tissue Factor. Blood 83: 3524, 1994.

9. Clarke BJ, Ofosu FA, Sridhara S, Bona RD, Rickles FR, Blajchman MA: The First Epidermal Growth Factor Domain of Human Coagulation Factor VII is Essential for Binding with Tissue Factor: FEBS Lett 298: 206, 1992.

10. Clarke BJ, Sridhara S: Incomplete Gamma Carboxylation of Human Coagulation Factor VII: Differential Effects on Tissue Factor Binding and Enzymatic Activity. Br J Haem 93: 445, 1996.

11. Davie EW, Fujikawa K, Kisiel W: The Coagulation Cascade: Initiation, Maintenance, and Regulation. Biochemistry 30: 10363, 1991.

12. Davie EW: Biochemical and Molecular Aspects of the Coagulation Cascade. Thromb Haem 74: 1, 1995.

13. Deng WP, Nickoloff JA: Site Directed Mutagenesis of Virtually any Plasmid by Eliminating a Unique Site. Anal Biochem 200: 81, 1992.

14. Dennis MS, Eigenbrot C, Skelton NJ, Ultsch MH, Santell L, Dwyer MA, O'Connell, Lazarus RA: Peptide Exosite Inhibitors of FVIIa as Anticoagulants. Nature 404: 465, 2000.

15. Dickinson CD, Kelly CR, Ruf W: Identification of Surface Residues Mediating Tissue Factor Binding and Catalytic Function of the Serine Protease Factor VIIa. Proc Nat Acad Sci USA 93: 14379, 1996.

16. Doolittle RF: The Evolution of Vertebrate Blood Coagulation: A Case of Yin and Yang. Thromb Haem 70: 24, 1993.

17. Edgington TS, Dickinson CD, Ruf W: The Structural Basis of the TF•FVIIa Complex in the Cellular Initiation of Blood Coagulation. Thromb Haem 78: 401, 1997.

18. Furie B, Furie BC: The Molecular Basis of Coagulation. Cell 53: 505, 1988.

19. Hagen FS, Gray CL, O'Hara P, Grant FJ, Saari GC, Wodbury RG, Hart CE, Insley M, Kisiel W, Kurachi K, Davie EW: Characterization of a cDNA Coding for Human Factor VII. Proc Natl Acad Sci USA 84: 5158, 1987.

20. Handford PA, Mayhew M, Baron M, Winship PR, Campbell ID, Brownlee GG: Key Residues Involved in Calcium-Binding Motifs in EGF-Like Domains. Nature 351: 164, 1991.

21. Higashi S, Nishimura H, Aital K, Iwanaga S: Identification of Regions of Bovine Factor VII Essential for Binding to Tissue Factor. J Biol Chem 269: 18891, 1994.

22. Idusogie E, Rosen E, Geng J-P, Carmeliet P, Calloen D, Castellino FJ: Characterization of a cDNA Encoding Murine Coagulation Factor VII. Thromb Haem 75: 481, 1996.

23. Iino M, Foster DC, Kisiel W: Functional Consequences of Mutations Ser-52 and Ser-60 in Human Blood Coagulation Factor VII. Arch Biochem Biophys 352: 182, 1998.

24. Janson TL, Stormorken H, Prydz H: Species Specificity of Tissue Thromboplastin. Haemostasis 14: 440, 1984.

25. Jin J, Chang J, Chang J-Y, Kelley RF, Stafford DW, Straight DL: Factor VIIa's First Epidermal Growth Factor-Like Domain's Role in Catalytic Activity. Biochemistry 38: 1185, 1999.

26. Kelly CR, Dickinson CD, Ruf: Ca^{2+} Binding to the First Epidermal Growth factor Module of Coagulation Factor VIIa is Important for Cofactor Interaction and Proteolytic Function. J Biol Chem 272: 17467, 1997.

27. Kirchhofer D, Nemerson Y: Initiation of Blood Coagulation: The Tissue Factor/Factor VIIa Complex. Curr Op Biotech 7: 386, 1996.

28. Leonard BJN, Chen Q, Blajchman MA, Ofosu FA, Sridhara S, Yang D, Clarke BJ: Factor VII Deficiency Caused by a Structural Variant N57D of the First Epidermal Growth factor Domain. Blood 91: 142, 1998.

29. Lin S-W, Smith KJ, Welsch D, Stafford DW: Expression and Characterization of Human Factor IX and Factor IX-Factor X Chimeras in Mouse C127 Cells. J Biol Chem 265: 144, 1990.

30. Mann KG, Nesheim ME, Church WR, Haley P, Krishnaswamy S: Surface-Dependent Reactions of the Vitamin K-Dependent Enzyme Complexes. Blood 76: 1, 1990.

31. McDonald JF, Shsh AM, Schwalbe RA, Kisiel W, Dhalback B, Nelsestuen GL: Comparison of Naturally Occurring Vitamin K-Dependent Proteins: Correlation of Amino Acid Sequences and Membrane Binding Properties Suggests a Membrane Contact Site. Biochemistry 36: 5120, 1997.

32. Mueller BM, Ruf W: Requirement for Binding of Catalytically Active Factor VIIa in Tissue Factor-Dependent Experimental Metastasis. J Clin Invest 101: 1372, 1998.

33. Muranyi A, Finn BE, Gippert GP, Forsen S, Stenflo J, Drakenberg T: Solution Structure of the N-Terminal EGF-Like Domain of Human Factor VII. Biochemistry 37: 10605, 1998.

34. Nishimura H, Kawabata S, Kisiel W, Hase S, Ikenaka T, Takao T, Shimonishi Y, Iwanaga S: Identification of a Disaccharide (Xyl-Glc) and a Trisaccharide (Xyl_2-Glc) *O*-Glycosidically Linked to a Serine Residue in the First Epidermal Growth Factor-

Like Domain of Human Factors VII and IX and Protein Z and Bovine Protein Z. J Biol Chem 264: 20320, 1989.

35. O'Brien DP, Kemball-Cook G, Hutchinson AM, Martin DMA, Johnson DJD, Byfield PGH, Takamiya O, Tuddenham EGD, McVey: Surface Plasmon Resonance Studies of the Interaction Between Factor VII and Tissue Factor. Demonstration of Defective Tissue Factor Binding in a Variant FVII Molecule (FVII-R79Q). Biochemistry 33:4162, 1994.

36. Paborsky LR, Tate KM, Harris RJ, Yansura DG, Band L, McCray G, Gorman CM, O'Brien DP, Chang JY, Swartz JR, Fung VP, Thomas JN, Vehar GA: Purification of Recombinant Human Tissue Factor. Biochemistry 28: 8072, 1989.

37. Patthy L: Evolution of the Proteases of Blood Coagulation and Fibrinolysis by Assambly from Modules. Cell 41: 657, 1985.

38. Patthy L: Modular design of Proteases of Coagulation, Fibrinolysis, and Complement Activation: Implications for Protein Engineering and Structure-Function Studies. Meth Enzymol 222, 10, 1993.

39. Patthy L: Introns and Exons. Curr Op Struct Biol 4: 383, 1994.

40. Perlak FJ: Single Step Large Scale Site-Directed *in vitro* Mutagenesis Using Multiple Oligonucleotides. Nuc Acids Res 18: 7457, 1990.

41. Rao Z, Handford P, Mayhew M, Knott V, Brownlee GG, Stuart D: The Structure of a Ca^{2+}-Binding Epidermal Growth Factor-Like Domain: Its Role in Protein-Protein Interactions. Cell 82: 131, 1995.

42. Ruf W, Rehemtulla A, Edgington TS: Phospholipid-independent and –dependent Interactions Required for Tissue Factor Receptor and Cofactor Function. J Biol Chem 266: 2158, 1991.

43. Ruf W: The Interaction of Activated Factor VII with Tissue Factor: Insight into the Mechanism of Cofactor-Mediated Activation of Activated Factor VII. Blood Coag Fibrin 9:S73, 1998.

44. Sambrook J, Fritsch EF, Maniatis T: Molecular Cloning – A Laboratory Manual. Cold Spring Harbor Laboratory Press, Plainview, NY, 1989.

45. Seligsohn U, Osterud, Rapaport SI: Coupled Amidolytic Assay for Factor VII: Its Use with a Clotting Assay to Determine the Activity State of Factor VII. Blood 5: 978, 1978.

46. Shah AM, Kisiel W, Foster DC, Nelsestuen GL: Manipulation of the Membrane Binding Site of Vitamin K-Dependent Proteins: Enhanced Biological Function of Human Factor VII. Proc Nat Acad Sci USA 95: 4229, 1998.

47. Sridhara S, Clarke BJ, Ofosu FA, High KA, Blajchman MA: The Direct Binding of Human Factor VII in Plasma to Recombinant Human Tissue Factor. Thromb Res 70: 307, 1993.

48. Sridhara S, Chiang S, High KA, Blajchman MA, Clarke BJ: Activation of a Recombinant Human Factor VII Structural Analogue Alters its Affinity of Binding to Tissue Factor. Am J Hematol 53: 66, 1996.

49. Stenflo J: Contributions of Gla and EGF-Like Domains to the Function of Vitamin K-Dependent Coagulation Factors. Crit Rev Euk Gene Exp 9: 59, 1999.

50. Stryer L: Biochemistry. W.H. Freeman and Company, New York, NY, 1995.

51. Sunnerhagen M, Olah GA, Stenflo J, Forsen Sm Drakenberg T, Trewhwlla J: The Relative Orientation of Gla and EGF Domains in Coagulation Factor X is Altered by Ca^{2+} Binding to the First EGF Domain. A Combined NMR-Small Angle X-ray Scattering Study. Biochemistry 35: 11547, 1996.

52. Tuddenham EGD, Pemberton S, Cooper DN: Inherited Factor VII Deficiency: Genetics and Molecular Pathology. Thromb Haem 74: 313, 1995.

53. Zhong D, Smith KJ, Birktoft JJ, Bajaj SP: First Epidermal Growth Factor-Like Domain of Human Blood Coagulation Factor IX is Required for Its Activation by Factor VIIa/Tissue Factor but Not by Factor XIa. Proc Natl Acad Sci USA 91: 3574, 1994.